

UNIVERSITY OF BIRMINGHAM

Research at Birmingham

The missing link in EBV immune evasion

Quinn, Laura; Williams, Luke; White, Claire; Forrest, Calum; Zuo, Jianmin; Rowe, Martin

DOI:

[10.1128/JVI.02183-15](https://doi.org/10.1128/JVI.02183-15)

License:

None: All rights reserved

Document Version

Peer reviewed version

Citation for published version (Harvard):

Quinn, LL, Williams, LR, White, C, Forrest, C, Zuo, J & Rowe, M 2015, 'The missing link in EBV immune evasion: the BDLF3 gene induces ubiquitination and downregulation of MHC class I and MHC class II', *Journal of virology*. <https://doi.org/10.1128/JVI.02183-15>

[Link to publication on Research at Birmingham portal](#)

Publisher Rights Statement:

Checked for eligibility: 10/12/2015

General rights

Unless a licence is specified above, all rights (including copyright and moral rights) in this document are retained by the authors and/or the copyright holders. The express permission of the copyright holder must be obtained for any use of this material other than for purposes permitted by law.

- Users may freely distribute the URL that is used to identify this publication.
- Users may download and/or print one copy of the publication from the University of Birmingham research portal for the purpose of private study or non-commercial research.
- User may use extracts from the document in line with the concept of 'fair dealing' under the Copyright, Designs and Patents Act 1988 (?)
- Users may not further distribute the material nor use it for the purposes of commercial gain.

Where a licence is displayed above, please note the terms and conditions of the licence govern your use of this document.

When citing, please reference the published version.

Take down policy

While the University of Birmingham exercises care and attention in making items available there are rare occasions when an item has been uploaded in error or has been deemed to be commercially or otherwise sensitive.

If you believe that this is the case for this document, please contact UBIRA@lists.bham.ac.uk providing details and we will remove access to the work immediately and investigate.

1 **The missing link in EBV immune evasion: the BDLF3 gene induces ubiquitination**
2 **and downregulation of MHC class I and MHC class II**

3 **Laura L Quinn, Luke R Williams, Claire White, Calum Forrest, Jianmin Zuo[#],**
4 **Martin Rowe**

5 Institute of Immunology & Immunotherapy (III), College of Medical & Dental Sciences,
6 University of Birmingham, B15 2TT, UK.

7 [#] Corresponding Author: email, J.Zuo@bham.ac.uk

8 Running Title: BDLF3, the missing link in EBV immune evasion

9 Abstract word count- 213

10 Main text word count- 5945

11 **Abstract**

12 The ability of Epstein-Barr virus (EBV) to spread and persist in human populations relies
13 on a balance between host immune responses and EBV immune-evasion. CD8⁺ cells
14 specific for EBV late lytic cycle antigens show poor recognition of target cells compared
15 to immediate early and early antigen-specific CD8⁺ cells. This phenomenon is in part
16 due to the early EBV protein, BILF1, whose immunosuppressive activity increases with
17 lytic cycle progression. However, published data suggest the existence of a hitherto
18 unidentified immune-evasion protein further enhancing protection against late EBV
19 antigen-specific CD8⁺ cells. We have now identified the late lytic gene, BDLF3, as the
20 missing link accounting for the efficient evasion during late lytic cycle. Interestingly,
21 BDLF3 also contributes to evasion of CD4⁺ cell responses to EBV. We report that
22 BDLF3 down-regulates expression of surface MHC class I and class II molecules in the
23 absence of any effect upon other surface molecules screened, including CD54 (ICAM-1)
24 and CD71 (Transferrin receptor). BDLF3 both enhanced internalization of surface MHC
25 molecules and reduced the rate of their appearance at the cell surface. The reduced
26 expression of surface MHC molecules correlated with functional protection against
27 CD8⁺ and CD4⁺ T cell recognition. The molecular mechanism was identified as BDLF3-
28 induced ubiquitination of MHC molecules and their subsequent downregulation in a
29 proteasomal dependent manner.

30

31 **Importance**

32 Immune-evasion is a necessary feature of viruses that establish life-long persistent
33 infections in the face of strong immune-responses. EBV is an important human
34 pathogen whose immune evasion mechanisms are only partly understood. Of the EBV
35 immune-evasion mechanisms identified to date, none could explain why CD8⁺ T cell
36 responses to late lytic cycle genes are so infrequent and, when present, recognize
37 lytically-infected target cells so poorly relative to CD8⁺ T cells specific for early lytic
38 cycle antigens. The present work identifies an additional immune-evasion protein,
39 BDLF3 that is expressed late in lytic cycle and impairs CD8⁺ T cell recognition by
40 targeting cell surface MHC class I molecules for ubiquitination and proteasomal
41 dependent downregulation. Interestingly, BDLF3 also targets MHC class II molecules, to
42 impair CD4⁺ T cell recognition. BDLF3 is therefore a rare example of a viral gene that
43 impairs both the class I and class II MHC antigen presenting pathways.

44

45 **Introduction**

46 Epstein-Barr virus (EBV) is a γ -herpesvirus found in more than 90% of the human
47 population. Primary infection with EBV is usually followed by establishment of lifelong
48 latent infection with occasional reactivation (1). The balance between host immune
49 responses, including $CD4^+$ and $CD8^+$ T cells, and viral immune evasion of these
50 responses is key to the spread and survival of EBV in human populations. Passive
51 evasion through the ability to establish antigenically silent latent infections is an
52 important characteristic of all herpesviruses, including EBV. In addition, active evasion
53 mechanisms are an important feature of herpesviruses. As these active evasion
54 mechanisms are predominantly observed during the lytic phase of the herpesvirus life-
55 cycle, they are presumed to be particularly important for enabling virus spread. There
56 have been a number of EBV encoded immune evasion genes identified that are
57 expressed in lytic cycle and target the MHC class I or class II antigen presentation
58 pathways (2, 3). Those genes responsible for interfering with MHC class I antigen
59 presentation include BGLF5, BNLF2a and BILF1 which each act upon different
60 elements of the MHC class I antigen presentation pathway (3-7). The EBV encoded
61 proteins BGLF5, BZLF1 and gp42 have been shown to interfere with MHC class II
62 antigen presentation (5, 8-10).

63 The above-mentioned MHC class I evasion genes encoded by EBV have been well
64 studied and shown to act via different mechanisms upon different elements of the MHC
65 class I antigen presentation pathway. Briefly, BGLF5 is a host shut off protein that has
66 been shown to induce the degradation of MHC class I mRNA, thereby reducing cell

67 surface MHC class I peptide presentation (5, 11). BILF1 is known to target both cell
68 surface MHC class I molecules and those on route to the surface for degradation thus
69 reducing the presentation of peptides to CD8⁺ T cells (7, 12, 13). Finally, BNLF2a
70 inhibits the function of the transporter associated with antigen processing (TAP), which
71 reduces the supply of peptides for loading on to MHC class I molecules, thus reducing
72 the level of MHC class I:peptide presentation to CD8⁺ T cells (4, 14, 15).

73 Our group recently investigated the relevance of BGLF5, BNLF2a and BILF1 immune
74 evasion genes in the context of lytic virus infection (16). It was concluded that BGLF5 in
75 fact plays a minimal role in protecting EBV infected cells against T cell recognition, and
76 that BNLF2a plays an important role of protecting cells during the immediate early and
77 early stages of lytic cycle, contributing little protection at late stage lytic cycle (IE>E>>L)
78 (14, 16). BILF1 was shown to contribute minimal protection during immediate early
79 stage lytic cycle, a reasonable level of protection during early stage lytic cycle and a
80 more dramatic level of protection was observed during late stage lytic cycle (IE<E<<L)
81 (16). This investigation revealed a level of co-operation between EBV encoded MHC
82 class I immune evasion genes in order to protect cells from CD8⁺ T cell recognition.
83 However, CD8⁺ T cell responses to late lytic cycle antigens still recognize lytically-
84 infected target cells relatively poorly, even in the absence of BILF1 expression. (16, 17).
85 This implies that another as yet unidentified immune evasion gene or genes may be
86 functioning late in lytic cycle.

87 In comparison to what is known about the immune evasion of MHC class I antigen
88 presentation, the evasion of MHC class II antigen presentation by EBV is less well

89 understood. Over-expression of the host shut off protein, BGLF5 has been shown to
90 result in a reduced level of surface MHC class II (5). In addition, the immediate early
91 protein BZLF1 has been shown to interfere with MHC class II antigen presentation by
92 modulating the expression of cell surface invariant chains (8). A third EBV encoded
93 gene, BZLF2 (gp42), has been shown to interfere with MHC class II antigen
94 presentation to CD4⁺ T cells by sterically hindering MHC class II interaction with the T
95 cell receptor, thus blocking CD4⁺ T cell recognition (9, 10). To date, no other EBV
96 proteins have been identified as potential CD4⁺ T cell immune evasion proteins.

97 The present study sought to identify novel candidate EBV genes responsible for
98 interfering with MHC class I antigen presentation during late phase lytic cycle, and thus
99 providing an explanation for the pronounced immune evasion observed at that stage in
100 the lytic cycle. Screening experiments revealed that the late lytic protein, BDLF3, whose
101 functions are unknown (18-20), was able to impair MHC class I antigen presentation.
102 Unexpectedly, BDLF3 also impaired CD4⁺ T cell recognition of MHC class II presented
103 peptides. The molecular mechanism for the effect of BDLF3 on antigen presentation
104 involved ubiquitination and proteasomal dependent downregulation of surface MHC
105 class I and class II molecules.

106

107 **Materials and methods**

108

109 **Plasmids**

110 The previously described (7) expression plasmid pCDNA3-IRES-GFP, a kind gift from
111 Professor Emmanuel Wiertz (Utrecht Medical Center, Netherlands), was used to
112 subclone and express a selection of EBV genes. The p509 expression plasmid for
113 BZLF1, a kind gift from Professor Paul Farrell (Imperial College London, UK), has also
114 been described (11) as has the cytoplasmic EBNA1 expression vector (21). The
115 retroviral plasmid PLZRS-NGFR, also a kind gift from Professor Emmanuel Wiertz, was
116 used to subclone PLZRS-BDLF3-NGFR and both were used in transient transfections to
117 allow for in house sorting of transfected cells, on the expression of surface truncated
118 nerve growth factor receptor (NGFR).

119

120 **Cells, transfections and electroporations**

121 The MJS (Mel JuSol) melanoma-derived cell line (22), and the EBV negative Burkitt
122 lymphoma cell line DG75 (23) were maintained in RPMI 1640 supplemented with 10%
123 fetal calf serum (FCS). CIITA-293 cells are HEK-293 cells stably expressing CIITA (24)
124 and were a kind gift from Dr Andrew Hislop, University of Birmingham. These were
125 maintained in Dulbecco's modified Eagle's medium (DMEM) supplemented with 10%
126 FCS. The myelogenous leukemia cell line K562, transduced to express either HLA-A2, -
127 B35, -Cw1, -DR or -DQ (a kind gift from Professor Emmanuel Wiertz, Utrecht) were
128 maintained in RPMI 1640 supplemented with 10% FCS plus 400µg/ml of geneticin
129 (Invitrogen). EBV specific CD4⁺ and CD8⁺ T cell clones were grown in RPMI 1640

130 supplemented with 10% FCS, 5% human serum, 30% supernatant from the interleukin-
131 2 producing MLA 144 cell line (25) and 50 U/ml recombinant interleukin-2, as described
132 previously (17).

133 Transient transfection of MJS and 293-CIITA cells with plasmid DNA was performed
134 using lipofectamine 2000 (Invitrogen) according to the manufacturer's instructions.

135 Transient expression of plasmid DNA using DG75 cells and K562 cells was performed
136 by electroporating cells at 290V and 950 μ F in 4mm gap cuvettes. In some experiments,
137 cells transiently transfected with NGFR expressing plasmids were positively selected for
138 the surface expression of NGFR using MACSelect NGFR-Transfected Cell Selection
139 kits, as per manufacturer's protocol (Miltenyi Biotec).

140

141 **Antibodies**

142 For immunoprecipitation experiments and for internalization/appearance assays,
143 unconjugated W6/32 and L243 murine monoclonal antibodies (MAbs) to human MHC
144 molecules were obtained from Biolegend: W6/32 (26) recognizes native β_2
145 microglobulin-associated MHC class I complexes (HLA-A, -B and -C alleles); and L243
146 for HLA-DR. For flow cytometry experiments, APC- and PE- conjugated antibodies to
147 HLA class I (W6/32), HLA-DR (L243), ICAM1/CD54 (HCD54) and transferrin
148 receptor/CD71 (TfR, CY1G4) were purchased from Biolegend. For western blotting,
149 mouse anti-ubiquitin antibody (P4D1) MAb was purchased from Biolegend. Goat
150 antibodies to calregulin were purchased from Santa Cruz Biotechnology. The BZ.1
151 murine MAb specific for the EBV BZLF1-encoded protein was generated by our

152 laboratory (27). The rabbit anti-BDLF3 (V8) serum was a kind gift from Dr. L.Hutt-
153 Fletcher (19).

154

155 **Flow cytometry analysis of cell surface MHC class I and class II molecules**

156 Cell surface expression of MHC class I and class II was determined by staining cells
157 with APC- or PE- conjugated anti-HLA class I or class II antibodies and detected on
158 BD biosciences Accuri C6 Flow Cytometer. Data were analyzed using FlowJo software
159 (TreeStar).

160 The kinetics of internalization and appearance of cell surface MHC molecules were
161 determined essentially as described previously (12). To assay the kinetics of surface
162 MHC class I and class II internalization, MJS cells were incubated on ice with saturating
163 amounts of anti-MHC class I (W6/32) or anti-MHC class II (L243) MAbs. Cells were then
164 washed three times in phosphate-buffered normal saline (PBS) and placed in culture
165 medium at 37°C for 60 mins. Aliquots of cells were taken at those times shown in
166 results, and were rapidly cooled to 0°C to inhibit further membrane trafficking. The level
167 of W6/32 or L243 MAb remaining at the cell surface was then analyzed by staining cells
168 with APC-conjugated goat anti-mouse IgG2a antibody (Biolegend). Cells were analyzed
169 using flow cytometry.

170 To assay the kinetics of MHC class I and II appearance, MJS cells were again
171 incubated with saturating amounts of W6/32 or L243 for 60 mins on ice. Cells were
172 washed three times in PBS and then placed in warm culture medium at 37°C for 60min,
173 cells were analyzed at times indicated in results. After cooling to 0°C, to prevent further
174 appearance of molecules at the surface through membrane trafficking, cells were

175 stained with APC-conjugated W6/32 or APC-conjugated L243 and analyzed using flow
176 cytometry. These directly conjugated anti-MHC detection antibodies will only bind to
177 MHC molecules that have appeared since the excess unconjugated blocking antibody
178 was washed away immediately prior to beginning the incubations in warmed medium.
179 Note that the MHC molecules newly-arrived at the cell surface are likely to be a mixture
180 of de-novo synthesized molecules arriving at the surface for the first time, and recycled
181 molecules that had previously been endocytosed.

182

183 **Flow cytometric analysis of whole cell (intracellular) proteins**

184 Intracellular staining for HLA class I and class II was performed to quantify the total
185 cellular levels of these proteins. Washed pellets of 0.5×10^6 cells were first fixed using
186 100 μ l Ebiosciences intracellular (IC) fixative for 1h on ice, followed by permeabilization
187 using 100 μ l (0.2%) Triton X-100 and further 30 min incubation on ice. After washing in
188 PBS, cells were incubated with appropriate conjugated antibody for 1h at 37°C. Cells
189 were then washed in PBS and analyzed using flow cytometry.

190

191 **T cell function assays**

192 'RAK' CD8⁺ T cell clones specific for the **RAKFKQLL** peptide originating from BZLF1
193 protein, and 'SNP' CD4⁺ clones specific for the **SNPKFENIAEGLRVLLARSH** epitope
194 from ENBA1 protein, were generated as previously described (16). Targets for RAK-
195 specific CD8⁺ T cells were generated by co-transfection of MJS cells with BZLF1 and
196 control-GFP or BDLF3-GFP expression plasmids. At 24h post transfection, cells were
197 used as targets for RAK specific CD8⁺ T cell clones. T cell recognition was determined

198 by interferon gamma (IFN- γ) enzyme-linked immunosorbant assay (ELISA) using a
199 previously described protocol (16). Targets for SNP-specific CD4⁺ T cell clones were
200 generated by transfection of MJS cells with the cytoplasmic EBNA1 expression plasmid,
201 EBNA1 Δ NLS, which generates a target protein that is efficiently processed via the MHC
202 antigen presentation pathway (21). At 24h post-transfection cells were re-seeded and
203 24h later these cells were transfected with control-NGFR or BDLF3-NGFR expression
204 plasmids. After a further 24h, cells were harvested and sorted as described above and
205 the recognition of these target cells by SNP-specific CD4⁺ T cell clones was determined
206 by IFN- γ ELISA.

207

208 **Immunoprecipitation**

209 Positively selected control-NGFR and BDLF3-NGFR expressing MJS cells (2×10^6) were
210 used for surface MHC class I and class II immunoprecipitation. Cells were incubated for
211 two hours on ice with anti-HLA class I Mab (W6/32) or anti-HLA class II Mab (L243),
212 then washed and lysed using 400 μ l of NP-40 buffer (0.5% Nonidet P-40, 5mM MgCl₂
213 and 50mM Tris-HCl, pH7.5) with protease inhibitor cocktail (Sigma P8340) at 4°C for 45
214 min. Nuclei and insoluble debris were removed by centrifugation, and the supernatants
215 were incubated with 20 μ l Dynabeads Protein A and 20 μ l Dynabeads Protein G
216 (Invitrogen) at 4°C overnight. Beads were then washed four times with NET buffer (0.5%
217 NP-40, 150mM NaCl₂, 5mM EDTA and 50mM Tris-HCl, pH 7.5) and the precipitated
218 proteins were eluted by boiling in reducing sample buffer for 5 min. Finally, samples
219 were separated by SDS-PAGE on 4-12 % Bis-Tris NuPage mini-gels with
220 morpholinepropanesulfonic acid (MOPS) electrolysis buffer (Invitrogen).

221 **Western blotting**

222 Total cell lysates were denatured in reducing sample buffer and then sonicated and
223 heated to 100°C for 5 min. Solubilized proteins equivalent to 2×10^5 cells/20 μ l sample
224 were separated by SDS-polyacrylamide gel electrophoresis (SDS-PAGE) on to 4-12%
225 acrylamide gradient bis-Tris NuPage minigels with MOPS running buffer (Invitrogen).

226

227 **Results**

228 **The late lytic gene BDLF3 is identified as an immune evasion protein**

229 As previously demonstrated, EBV encodes a number of immune evasion genes that co-
230 operate to afford the protection of EBV infected cells against recognition by CD8⁺ T cells
231 during lytic cycle. However, it has been hypothesized that an as yet unidentified EBV
232 lytic gene may be responsible for the ultimate protection of EBV infected cells during
233 late lytic cycle (16). In order to identify other potential EBV immune evasion proteins
234 involved in protecting infected cells against CD8⁺ T cell recognition, more than 25 EBV
235 genes expressed during lytic cycle were transiently expressed in MJS cells using
236 bicistronic plasmid vectors that co-expressed GFP with the test gene (Supplementary
237 Fig. 1A). The expression of GFP protein allowed for the identification of transfected cells
238 using flow cytometry. At 24h post-transfection, flow cytometric analysis was used to
239 analyse surface expression levels of MHC class I on GFP positive cells. Of all EBV lytic
240 genes included in this screen the only protein that reproducibly affected surface levels
241 of MHC class I was BDLF3 (Fig. 1A). Fig. 1A shows a representative selection of these
242 screens. As a control, the level of surface MHC class II was also analyzed in this screen
243 (Supplementary Fig. 1B). Interestingly, BDLF3 also affected the surface expression of
244 MHC class II (Fig. 1B).

245 BDLF3 has previously been classified as a late expressed lytic protein (19). We
246 confirmed the late expression kinetics using the EBV positive cell line, AKBM (9) that
247 can be induced in to lytic cycle by cross linking of the B cell receptor. Following
248 induction, aliquots of induced AKBM cells were taken at 0h, 1h, 6h, 12h, 24h, and 48h

249 time points and immunoblotting was performed in order to detect the expression of
250 BDLF3 and the immediate early protein BZLF1. As shown in Fig. 1C, BDLF3 protein
251 expression is detected weakly at 12hr post induction but with stronger expression seen
252 at 24hr. These expression kinetics are consistent with previous findings (19) and
253 suggests that BDLF3 could potentially be the 'missing link' immune evasion protein
254 responsible for interfering with MHC class I antigen presentation during late stage lytic
255 cycle to protect these cells against CD8⁺ T cell recognition. In addition, the effect on
256 expression of MHC class II molecules raised the possibility that BDLF3 also plays a role
257 in CD4⁺ T cell immune evasion. To confirm that the levels of BDLF3 protein expression
258 in our transfected cells were physiologically relevant, BDLF3 protein expression levels
259 in the transfected MJS cells was compared with BDLF3 expression level in induced
260 AKBM cells after adjusting for the percentage of GFP⁺ cells in MJS cells and
261 percentage of VCA⁺ cells in induced AKBM cells. Quantification of western blots
262 (Supplementary Fig. 2) showed that the expression of BDLF3 in MJS was around 70%
263 of that expressed in induced AKBM cells.

264 In order to confirm that BDLF3 acts specifically on MHC class I and MHC class II, MJS
265 cells transiently expressing BDLF3 were harvested at 24hr post-transfection and were
266 analyzed in more detail using flow cytometry to detect surface levels of MHC class I,
267 MHC class II, and other cell surface proteins. The results in Fig. 2A indicated that
268 BDLF3 expressing cells (dashed line) exhibit a 60% decrease in surface MHC class I
269 mean fluorescence intensity (MFI) compared to control cells (solid black line). A similar
270 result was observed for surface levels of MHC class II on BDLF3 positive cells (Fig. 2B),
271 where there was a reduction of 50% in MHC class II MFI. Importantly, the levels two

272 other surface proteins tested, Transferrin receptor (TfR; Fig. 2C) and ICAM1, (Fig. 2D)
273 were not affected by the expression of BDLF3.

274 Since B cells are the natural reservoir for EBV, we next investigated the phenotype of
275 BDLF3 in B cells. To this end, the effect of transient BDLF3 expression on surface MHC
276 molecules on the EBV negative B cell line, DG75 was investigated using flow cytometry.
277 In this instance, the control of ICAM1 could not be included as its expression on DG75
278 cells is negligible; therefore the effect of BDLF3 on expression of CD19 was analyzed
279 along with TfR expression. As shown in Fig. 2E-H, results similar to those seen in MJS
280 cells were obtained. BDLF3 expressing DG75 cells showed a 43% reduction in the MFI
281 of MHC class I (Fig. 2E) and a 30% reduction in MHC class II (Fig. 2F) compared to
282 control cells not expressing BDLF3. There was no observed effect of BDLF3 on the
283 expression of surface TfR (Fig. 2G) or CD19 (Fig. 2H).

284

285 **BDLF3 induces downregulation of all screened MHC class I and MHC class II** 286 **alleles**

287 Since some viral immune evasion genes, including BILF1, have been shown to
288 preferentially target specific HLA class I alleles (13), we next sought to investigate the
289 HLA-specificity of BDLF3. To do so, MHC class I negative K562 cells engineered to
290 stably express HLA-A2, -B35 or -Cw1 were transiently transfected to express either
291 BDLF3 or a control vector. At 24h post-transfection the surface level HLA-A2, -B35 and
292 -Cw1 on positively transfected cells was detected using flow cytometry. As shown in
293 Fig. 3A, cells expressing BDLF3 showed a decrease in the cell surface level of HLA-A2

294 (upper histograms) (27% reduction in MFI), HLA-B35 (middle histograms) (34%
295 reduction in MFI) and HLA-Cw1 (lower histograms) (26% reduction in MFI) compared to
296 control cells. A similar approach was then used to test the specificity of BDLF3 for HLA
297 class II alleles. Here, HLA class II negative HEK-293 cells engineered to stably
298 expressing CIITA, thus driving the surface expression of HLA-DR and -DQ, were
299 transiently transfected to express BDLF3 or control vector. Similar to that seen for HLA
300 class I alleles, BDLF3 induced a reduction in both HLA-DR (47% reduction in MFI) (Fig.
301 3B, upper histograms) and HLA DQ (32% reduction in MFI) (Fig. 3B, lower histograms)
302 compared to control transfected cells. In all examples the level of surface TfR remained
303 similar between BDLF3 and control transfected cells (data not shown). These results
304 indicate that BDLF3 is not selective in down-regulating HLA molecules but instead acts
305 more broadly to down regulate all HLA class I and HLA class II molecules.

306

307 **BDLF3 mediated reductions in surface MHC class I and class II confers protection**
308 **against both CD8⁺ and CD4⁺ T cell recognition**

309 Since BDLF3 induces a reduction in the level of surface MHC class I and class II
310 molecules, we next investigated whether BDLF3 expression provided protection against
311 recognition by EBV-specific CD8⁺ and CD4⁺ T cells. In order to address this, the HLA-
312 B8 positive cell line MJS cells, were co-transfected with BZLF1 and either BDLF3-GFP
313 or control-GFP vector plasmids (Fig. 4A). At 24h post-transfection these cells were used
314 as targets in a T cell assay with CD8⁺ T cell clones restricted through HLA-B8 and
315 specific for the peptide RAKFKQLL, contained within the BZLF1 antigen. T cell

316 recognition was measured as IFN- γ release using IFN- γ ELISA. As shown in one
317 representative experiment (n=3) in Fig. 4A, the expression of BDLF3 resulted in a
318 significant decrease in IFN- γ release by RAK-specific T cell clones, from ~1100pg/ml to
319 ~500pg/ml. The BDLF3-mediated reduction in BZLF1-specific CD8⁺ T cell recognition
320 was not due to any change in the expression of BZLF1 target protein expression (Fig.
321 4B).

322 In order to investigate the ability of BDLF3 to protect cells against recognition by CD4⁺ T
323 cells, a similar method was employed. Here, MJS cells stably expressing the HLA class
324 II allele DR51 were transfected to express cytoplasmic EBNA1 for 48h and either
325 BDLF3-NGFR or control-NGFR vector for a further 24hr (Fig. 4C). Cells were then
326 sorted on expression of NGFR and subsequently used as targets for a CD4⁺ T cell
327 clones specific for the HLA-DR51 restricted epitope SNPKFENIAEGLRVLLARSH,
328 contained within EBNA1. As shown in Fig. 4C, the expression of BDLF3 resulted in a
329 decrease in T cell recognition (IFN- γ release) by SNP-specific CD4⁺ T cell clones from
330 ~1300pg/ml to ~900pg/ml, compared to control cells. The BDLF3-mediated reduction in
331 EBNA1-specific CD4⁺ T cell recognition was not due to any change in the expression of
332 EBNA1 target protein expression (Fig. 4D). Thus, in a similar pattern to those results
333 seen for BDLF3 protection against CD8⁺ T cell recognition, BDLF3 induced reduction in
334 surface MHC class II molecules also correlated with protection against CD4⁺ T cell
335 recognition.

336 These data show that BDLF3 induced reduction in cell surface MHC class I and class II
337 is functional in protecting BDLF3 expressing cells against recognition by both CD8⁺ and
338 CD4⁺ T cells.

339 **BDLF3 downregulates surface MHC molecules more dramatically than total MHC**
340 **molecules**

341 To explore the mechanism of MHC class I and class II downregulation by BDLF3, we
342 first asked whether the total cellular pool of MHC molecules was affected, or whether
343 surface MHC molecules were selectively targeted. To this end, flow cytometry of
344 intracellular staining of fixed and permeabilized cells was used to detect the level of
345 whole cell MHC molecules compared to surface MHC molecules detected on
346 impermeable viable cells. As expected, surface level MFI of MHC class I and class II
347 were both reduced by approximately 50% on cells expressing BDLF3 compared to
348 control cells (Fig. 5A, left-hand column). This difference was found to be significant (Fig.
349 5B, white bars). Interestingly, there was only a slight decrease of 10% in the MFI of
350 whole cell MHC class I and MHC class II compared to control cells (Fig. 5A, right
351 column) and this small reduction was not statistically significant when the results from
352 three independent experiments were pooled and analyzed (Fig. 5B, grey bars). To
353 confirm these findings by an independent method, control GFP expressing MJS and
354 BDLF3-GFP expressing MJS cells were purified using Mo-flow cell sorter and the
355 expression of total MHC-I and MHC-II was examined by western-blot. The result
356 showed no significant difference (supplementary Fig.3), confirming the result from

357 intracellular flow cytometry data. Importantly, BDLF3 had no effect on surface or whole
358 cell levels of ICAM1 expression (Figs. 5A and 5B, bottom panel).

359 These data show that BDLF3 affects the levels of surface MHC molecules more
360 dramatically than it affects whole cell MHC molecules, suggesting that BDLF3 exerts its
361 function predominantly on surface MHC class I and II rather than the intracellular
362 fraction of these molecules.

363

364 **BDLF3 induces rapid internalization and delayed appearance of MHC molecules**

365 Since BDLF3 predominantly targets surface MHC molecules, we next examined
366 whether it targets those MHC molecules already at the cell surface or those trafficking to
367 the cell surface. We therefore compared the kinetics of MHC class I and class II
368 internalization and appearance at the cell surface of BDLF3 expressing cells using flow
369 cytometry. Representative examples are shown of MHC class I (Fig. 6A, upper) and
370 class II (Fig. 6A, lower) internalization assays, where the percentage of MHC class I and
371 class II remaining on the surface of BDLF3 expressing and control cells was measured
372 over 60 minutes. Cells expressing BDLF3 showed lower levels of surface MHC
373 remaining at the cell surface at each time point indicated, such that by 60min there were
374 respectively 20% and 13% less surface MHC class I and MHC class II on BDLF3
375 expressing cells compared to control cells. These data indicate that BDLF3 induces a
376 more rapid rate of both MHC class I and MHC class II internalization.

377 When a similar assay was used to measure the rate of MHC class I and class II surface
378 appearance, BDLF3 expressing cells conversely showed a decreased rate of both MHC
379 class I and class II surface appearance at each time point compared to control cells
380 (Fig. 6B). By 60 min, the appearance of MHC class I and class II on BDLF3 expressing
381 cells at time point 60min was reduced by 50% and 47% respectively in comparison to
382 control cells. This BDLF3-mediated reduction in the rate of appearance of MHC at the
383 surface (Fig. 6B) was noticeably greater than the accelerated rate of endocytosis
384 (Fig.6A).

385 It should be noted that in all experiments rate of TfR internalization or appearance
386 remained similar between control and BDLF3 expressing cells (data not shown). These
387 data indicate that BDLF3 is able to both enhance endocytosis of MHC molecules at the
388 cell surface and interfere with the trafficking of intracellular MHC molecules to the cell
389 surface.

390

391 **BDLF3 downregulation of surface MHC molecules involves ubiquitination and the** 392 **proteasomal pathway**

393 We next sought to identify the mechanism by which BDLF3 is able to enhance
394 internalization and delay the appearance of surface MHC class I and MHC class II
395 molecules. Our initial experiments were designed to identify which pathway BDLF3
396 might utilize in order to reduce the expression of surface MHC molecules. To this end,
397 we incubated BDLF3 expressing cells with proteasomal and lysosomal inhibitors. In the
398 absence of drug treatment, cells expressing BDLF3 showed lower levels of surface

399 MHC class I and II expression compared to control cells (Fig. 7A) as expected.
400 However, when incubated with the proteasomal inhibitor, MG132, BDLF3 expressing
401 cells showed no such reduction in surface MHC class I and MHC class II levels
402 compared to control cells (Fig. 7B). Part abrogation of BDLF3 phenotype by MG132
403 was observed after 4hr treatment, but the effect of MG132 treatment was maximal after
404 16h (Supplementary Fig. 4). Similar results were seen when cells were treated with a
405 second proteasomal inhibitor, bortezomib (Supplementary Fig. 5), whereas treatment
406 with a lysosomal inhibitor, bafilomycin (Supplementary Fig. 6), did not prevent BDLF3
407 induced downregulation of surface MHC molecules. These data indicate that BDLF3
408 induced downregulation of surface MHC molecules is dependent upon the proteasomal
409 pathway.

410 As BDLF3 downregulates surface MHC molecules through increased internalization and
411 delayed appearance (Fig. 6), we next examined what effect proteasomal inhibition might
412 have on the kinetics of MHC class I and class II internalization and appearance at the
413 cell surface of BDLF3 expressing cells. The results showed that MG132 completely
414 abrogated the effect of BDLF3 on both the rate of internalization (Fig 7C) and the rate of
415 appearance (Fig.7D), demonstrating an essential role of the proteasome in BDLF3
416 induced MHC molecule downregulation.

417

418 Given the essential role that the proteasome plays in BDLF3 induced reduction of
419 surface MHC molecules, and that ubiquitination is an important component of the
420 proteasomal pathway, we next assessed whether BDLF3 induces ubiquitination of

421 surface MHC molecules. To this end, MJS cells were transfected with various
422 expression vectors including BDLF3, control vector and ubiquitin (Fig. 7E, F). These
423 cells were then incubated with or without the proteasomal inhibitor, MG132. At 24h post-
424 transfection, surface MHC class I or MHC class II molecules were immunoprecipitated
425 from BDLF3 expressing or control cells and resulting immunoblots were probed with
426 ubiquitin-specific antibodies. As shown in Fig. 7, poly-ubiquitinated high molecular
427 weight bands appeared in immunoblots for immunoprecipitated MHC class I (Fig. 7E)
428 and MHC class II (Fig. 7F) in BDLF3 expressing cells treated with MG132. These
429 ubiquitin-reactive bands were less pronounced both in control cells treated with MG132
430 and in BDLF3-expressing cells not treated with MG132.

431 **Discussion**

432 This study reveals the identity and mechanism of novel immune evasion gene, BDLF3,
433 which induces downregulation of not only cell surface MHC class I but also MHC class
434 II, to the extent that antigen recognition by both CD8⁺ and CD4⁺ virus-specific T cells is
435 functionally impaired. The BDLF3 protein was first identified a number of years ago as
436 the glycoprotein gp150, which is located at the cell membrane and in the virion, is not
437 essential for EBV replication, and hitherto had no known function (18-20). Our study
438 now allows a function to be assigned to the BDLF3 protein.

439 The identification of BDLF3 as an immune evasion protein has an important impact on
440 our knowledge of the T cell response to lytic EBV antigens and the protection of EBV
441 infected cells from recognition by these T cells. EBV lytic cycle involves the
442 synchronous expression of more than 60 viral proteins, many of which elicit strong CD4⁺
443 and CD8⁺ T cell responses, but various immune-evasion mechanisms enable EBV to
444 persist as a lifelong infection. For CD8⁺ T cell responses to lytic cycle antigens, there is
445 a pattern of immunodominance that correlates with the efficiency of antigen
446 presentation during lytic cycle. An earlier study by our group revealed that the known
447 immune evasion genes, BGLF5, BNLF2a and BILF1 act in co-operation to afford
448 protection to EBV infected cells against lytic specific CD8 T⁺ cell recognition. However,
449 the ultimate protection that is seen in late phase lytic cycle could not be fully explained
450 by the action of these known evasion genes (16). The identification of BDLF3, which is
451 expressed during late stage lytic cycle, as a potent inhibitor of the MHC class I antigen
452 presentation pathway makes it a prime candidate for the 'missing link' immune evasion

453 protein responsible for protecting EBV infected cells from CD8⁺ T cell responses during
454 late stage lytic cycle.

455 Another important feature of BDLF3 is its ability to induce MHC class II downregulation
456 and evade CD4⁺ T cell recognition. Evidence is accumulating in the literature showing
457 that viruses target multiple points on the MHC class II antigen presentation pathway,
458 including: suppression of CIITA (28, 29), diversion or degradation of DR molecules
459 during membrane transport (30) and direct targeting of the CD74 (invariant chain)
460 chaperone of DR (8). Two viral genes expressed during EBV lytic cycle have been
461 reported to manipulate MHC class II antigen presentation pathway. BZLF1 induces a
462 marked downregulation of surface CD74 to impair antigen presentation and CD4⁺ T cell
463 recognition (8), and Gp42 sterically inhibits interactions between TCR on the CD4⁺ T
464 cell with MHC-II peptide complexes (10). The identification of BDLF3 as a novel MHC
465 class II evasion gene from EBV indicates that, similarly to interference with MHC class I
466 antigen presentation, interference with MHC class II antigen presentation very likely
467 involves the cooperative action of multiple evasion genes.

468 The fact that BDLF3 is an EBV late lytic cycle protein, suggests that it would help to
469 provide enhanced protection of the virus-producing cells prior to release of mature
470 virions. In addition, as BDLF3 can be detected in the EBV virion (31), this raises the
471 possibility that BDLF3 can act immediately after new infections of B cells to modulate
472 recognition by existing EBV specific CD4⁺ T cells. Considering the important role of
473 MHC class II molecules and gp42 in EBV infection, and also the observation that
474 BDLF3 knock-out EBV virus particles can infect epithelial cells better than B cells (18),

475 we can propose a potential role of BDLF3 in the EBV infection. BDLF3 expression
476 results in decreased MHC class II expression at the surface of lytically replicating cells,
477 reducing the amount of MHC class II available to bind gp42. We would therefore predict
478 that BDLF3 knockout virions may contain less envelope gp42 than wild type EBV, with a
479 consequent enhanced ability to infect epithelial cells.

480 Our data indicate that the mechanism of BDLF3 interference with the appearance of
481 MHC molecules at, and internalization from, the cell surface, involves ubiquitination of
482 MHC molecules and proteasome-dependent pathways. The targeting of MHC
483 molecules for ubiquitination has been described for other viral immune evasion proteins,
484 but the mechanism of action of BDLF3 is clearly distinct. An example is the K3 and K5
485 proteins encoded by Kaposi's sarcoma-associated herpesvirus (KSHV), which function
486 as two membrane-bound E3 ubiquitin ligases and have been shown to facilitate the
487 rapid endocytosis and subsequent degradation of MHC class I by inducing
488 ubiquitination (32-37). Unlike K3 and K5, there is no evidence to show that BDLF3 itself
489 is an E3 ubiquitin ligase, therefore it is very likely that BDLF3 functions via a different
490 mechanism. Indeed in terms of the MHC class I downregulation, BDLF3 can affect all
491 MHC class I alleles we studied, whereas K5 affects HLA-A and -B but has a weak
492 effect on HLA-C, while K3 downregulates all HLA class I alleles (33). More importantly,
493 KSHV K3 and K5 can downregulate a range of other surface proteins including B7-2,
494 CD54 (ICAM-1), CD1d, CD31 (PECAM-1), IFN- γ R1, MICA/B, BST-2, ALCAM, Syntaxin-
495 4 (38-42). In contrast we found that BDLF3 targets MHC-I and MHC-II, but not CD54
496 (Fig. 2) or MICA/B (data not shown). Another distinguishing feature of BDLF3 is that
497 whilst the surface levels of MHC class I and class II were reduced by around 50%, there

498 was a minimal decrease of whole cell MHC class I and MHC class II (Fig. 5A, and
499 Supplementary Fig. 3). That BDLF3 can induce a 50% reduction in surface MHC
500 molecules against a reduction of less than 10% of the whole cell MHC molecules
501 reflects the fact that there is relatively large reservoir of MHC class I and MHC class II
502 inside the cells. Therefore, the 10% reduction in whole cell MHC class I and II could
503 represent the complete degradation of the 50% of MHC class I and II that is lost from
504 the surface in the presence of BDLF3.

505 Whilst BDLF3 does not function as ubiquitin E3 ligase, it does nevertheless
506 downregulate surface MHC class I and MHC class II through inducing ubiquitination.
507 How might this be? One possible explanation is that it may recruit other cellular E3
508 ubiquitin ligase proteins such as members of the membrane-associated RING-CH
509 (MARCH) proteins, the cellular orthologues of K3 and K5. These proteins have been
510 implicated in the regulation of cell surface molecules including MHC class I, MHC class
511 II, ICAM and transferrin receptor (36, 43-46). Indeed, the overexpression of MARCH-IV
512 and MARCH-IX proteins induces ubiquitination and rapid internalization of MHC class I
513 (43). Numerous MARCH proteins have been identified that target MHC class I or MHC
514 class II although, at the time of writing, no single known MARCH protein induces the
515 ubiquitination of both MHC class I and class II without affecting other surface markers
516 that are left unaffected by BDLF3 (47). Our preliminary experiments have not been able
517 to demonstrate co-immunoprecipitation of MHC molecules with BDLF3 (data not shown).
518 Thus BDLF3 may recruit an as of yet unidentified MARCH family protein or perhaps
519 several of these proteins. If so, then the specificity of BDLF3 would be due to the target

520 molecules of these recruited proteins. Future work will be aimed at resolving these
521 possibilities.

522 Considering the data that we have obtained for BDLF3, and the features that distinguish
523 the effects of BDLF3 from previously characterized immune evasion proteins, we
524 postulate that its mechanism of action is broadly as follows. As BDLF3 reduces the rate
525 of appearance of MHC molecules at the cell surface to a greater extent than it increases
526 the rate of endocytosis (Fig.6) we suppose that the reduced rate of appearance must be
527 due at least in part to an effect on de novo synthesized MHC molecules trafficking to the
528 surface. Therefore, BDLF3 targets for ubiquitination both de novo synthesized and
529 recycling endocytosed MHC molecules. These ubiquitinated MHC molecules are
530 directed for proteasomal degradation or, in the presence of proteasomal inhibitors,
531 accumulate at the cell surface. The finer details of the biochemical mechanisms, and
532 the identity of the ubiquitin ligases involved, remain to be resolved.

533 The acquisition of immune evasion proteins has played a critical role in the evolution of
534 viruses. It is interesting to note that an EBV homolog, the marmoset lymphocryptovirus
535 (maLCV), which naturally infects new world nonhuman primates, lacks BDLF3. This
536 may be relevant to the fact that serological studies reveal maLCV infection in
537 marmosets to be much less ubiquitous than EBV in humans (48, 49). It might therefore
538 be speculated that the acquisition of BDLF3 immune evasion functions is a later
539 evolutionary event that contributes to the success of EBV in successfully colonizing the
540 vast majority of the human population.

541 **Reference**

- 542 1. **Rickinson AB, E. Kieff.** 2007. Epstein-Barr Virus. In D. M. Knipe and P. M. Howley (ed.), *Fields*
543 *Virology* **2**. Lippincott Williams & Wilkins, Philadelphia, PA:2655-2700. .
- 544 2. **Ressing ME, Horst D, Griffin BD, Tellam J, Zuo J, Khanna R, Rowe M, Wiertz EJ.** 2008. Epstein-
545 Barr virus evasion of CD8(+) and CD4(+) T cell immunity via concerted actions of multiple gene
546 products. *Semin Cancer Biol* **18**:397-408.
- 547 3. **Rowe M, Zuo J.** 2010. Immune responses to Epstein-Barr virus: molecular interactions in the
548 virus evasion of CD8+ T cell immunity. *Microbes Infect* **12**:173-181.
- 549 4. **Hislop AD, Ressing ME, van Leeuwen D, Pudney VA, Horst D, Koppers-Lalic D, Croft NP, Neefjes**
550 **JJ, Rickinson AB, Wiertz EJ.** 2007. A CD8+ T cell immune evasion protein specific to Epstein-Barr
551 virus and its close relatives in Old World primates. *J Exp Med* **204**:1863-1873.
- 552 5. **Rowe M, Glaunsinger B, van Leeuwen D, Zuo J, Sweetman D, Ganem D, Middeldorp J, Wiertz**
553 **EJ, Ressing ME.** 2007. Host shutoff during productive Epstein-Barr virus infection is mediated by
554 BGLF5 and may contribute to immune evasion. *Proc Natl Acad Sci U S A* **104**:3366-3371.
- 555 6. **Zeidler R, Eissner G, Meissner P, Uebel S, Tampe R, Lazis S, Hammerschmidt W.** 1997.
556 Downregulation of TAP1 in B lymphocytes by cellular and Epstein-Barr virus-encoded
557 interleukin-10. *Blood* **90**:2390-2397.
- 558 7. **Zuo J, Currin A, Griffin BD, Shannon-Lowe C, Thomas WA, Ressing ME, Wiertz EJ, Rowe M.**
559 2009. The Epstein-Barr virus G-protein-coupled receptor contributes to immune evasion by
560 targeting MHC class I molecules for degradation. *PLoS Pathog* **5**:2.
- 561 8. **Zuo J, Thomas WA, Haigh TA, Fitzsimmons L, Long HM, Hislop AD, Taylor GS, Rowe M.** 2011.
562 Epstein-Barr virus evades CD4+ T cell responses in lytic cycle through BZLF1-mediated
563 downregulation of CD74 and the cooperation of vBcl-2. *PLoS Pathog* **7**:22.
- 564 9. **Ressing ME, van Leeuwen D, Verreck FA, Keating S, Gomez R, Franken KL, Ottenhoff TH,**
565 **Spriggs M, Schumacher TN, Hutt-Fletcher LM, Rowe M, Wiertz EJ.** 2005. Epstein-Barr virus gp42
566 is posttranslationally modified to produce soluble gp42 that mediates HLA class II immune
567 evasion. *J Virol* **79**:841-852.
- 568 10. **Ressing ME, van Leeuwen D, Verreck FA, Gomez R, Hemskerk B, Toebes M, Mullen MM,**
569 **Jardetzky TS, Longnecker R, Schilham MW, Ottenhoff TH, Neefjes J, Schumacher TN, Hutt-**
570 **Fletcher LM, Wiertz EJ.** 2003. Interference with T cell receptor-HLA-DR interactions by Epstein-
571 Barr virus gp42 results in reduced T helper cell recognition. *Proc Natl Acad Sci U S A* **100**:11583-
572 11588.
- 573 11. **Zuo J, Thomas W, van Leeuwen D, Middeldorp JM, Wiertz EJ, Ressing ME, Rowe M.** 2008. The
574 DNase of gammaherpesviruses impairs recognition by virus-specific CD8+ T cells through an
575 additional host shutoff function. *J Virol* **82**:2385-2393.
- 576 12. **Zuo J, Quinn LL, Tamblyn J, Thomas WA, Federle R, Delecluse HJ, Hislop AD, Rowe M.** 2011.
577 The Epstein-Barr virus-encoded BILF1 protein modulates immune recognition of endogenously
578 processed antigen by targeting major histocompatibility complex class I molecules trafficking on
579 both the exocytic and endocytic pathways. *J Virol* **85**:1604-1614.
- 580 13. **Griffin BD, Gram AM, Mulder A, Van Leeuwen D, Claas FH, Wang F, Ressing ME, Wiertz E.**
581 2013. EBV BILF1 evolved to downregulate cell surface display of a wide range of HLA class I
582 molecules through their cytoplasmic tail. *J Immunol* **190**:1672-1684.
- 583 14. **Croft NP, Shannon-Lowe C, Bell AI, Horst D, Kremmer E, Ressing ME, Wiertz EJ, Middeldorp**
584 **JM, Rowe M, Rickinson AB, Hislop AD.** 2009. Stage-specific inhibition of MHC class I
585 presentation by the Epstein-Barr virus BNLF2a protein during virus lytic cycle. *PLoS Pathog* **5**:26.

- 586 15. **Horst D, van Leeuwen D, Croft NP, Garstka MA, Hislop AD, Kremmer E, Rickinson AB, Wiertz**
587 **EJ, Ressing ME.** 2009. Specific targeting of the EBV lytic phase protein BNLF2a to the transporter
588 associated with antigen processing results in impairment of HLA class I-restricted antigen
589 presentation. *J Immunol* **182**:2313-2324.
- 590 16. **Quinn LL, Zuo J, Abbott RJ, Shannon-Lowe C, Tierney RJ, Hislop AD, Rowe M.** 2014.
591 Cooperation between Epstein-Barr virus immune evasion proteins spreads protection from
592 CD8+ T cell recognition across all three phases of the lytic cycle. *PLoS Pathog* **10**.
- 593 17. **Pudney VA, Leese AM, Rickinson AB, Hislop AD.** 2005. CD8+ immunodominance among
594 Epstein-Barr virus lytic cycle antigens directly reflects the efficiency of antigen presentation in
595 lytically infected cells. *J Exp Med* **201**:349-360.
- 596 18. **Borza CM, Hutt-Fletcher LM.** 1998. Epstein-Barr virus recombinant lacking expression of
597 glycoprotein gp150 infects B cells normally but is enhanced for infection of epithelial cells. *J Virol*
598 **72**:7577-7582.
- 599 19. **Kurilla MG, Heineman T, Davenport LC, Kieff E, Hutt-Fletcher LM.** 1995. A novel Epstein-Barr
600 virus glycoprotein gp150 expressed from the BDLF3 open reading frame. *Virology* **209**:108-121.
- 601 20. **Nolan LA, Morgan AJ.** 1995. The Epstein-Barr virus open reading frame BDLF3 codes for a 100-
602 150 kDa glycoprotein. *J Gen Virol* **76**:1381-1392.
- 603 21. **Leung CS, Haigh TA, Mackay LK, Rickinson AB, Taylor GS.** 2010. Nuclear location of an
604 endogenously expressed antigen, EBNA1, restricts access to macroautophagy and the range of
605 CD4 epitope display. *Proc Natl Acad Sci U S A* **107**:2165-2170.
- 606 22. **Johnson JP, Demmer-Dieckmann M, Meo T, Hadam MR, Riethmuller G.** 1981. Surface antigens
607 of human melanoma cells defined by monoclonal antibodies. I. Biochemical characterization of
608 two antigens found on cell lines and fresh tumors of diverse tissue origin. *Eur J Immunol* **11**:825-
609 831.
- 610 23. **Ben-Bassat H, Goldblum N, Mitrani S, Goldblum T, Yoffey JM, Cohen MM, Bentwich Z, Ramot**
611 **B, Klein E, Klein G.** 1977. Establishment in continuous culture of a new type of lymphocyte from
612 a "Burkitt like" malignant lymphoma (line D.G.-75). *Int J Cancer* **19**:27-33.
- 613 24. **Sabbah S, Jagne YJ, Zuo J, de Silva T, Ahasan MM, Brander C, Rowland-Jones S, Flanagan KL,**
614 **Hislop AD.** 2012. T-cell immunity to Kaposi sarcoma-associated herpesvirus: recognition of
615 primary effusion lymphoma by LANA-specific CD4+ T cells. *Blood* **119**:2083-2092.
- 616 25. **Rabin H, Hopkins RF, 3rd, Ruscetti FW, Neubauer RH, Brown RL, Kawakami TG.** 1981.
617 Spontaneous release of a factor with properties of T cell growth factor from a continuous line of
618 primate tumor T cells. *J Immunol* **127**:1852-1856.
- 619 26. **Barnstable CJ, Bodmer WF, Brown G, Galfre G, Milstein C, Williams AF, Ziegler A.** 1978.
620 Production of monoclonal antibodies to group A erythrocytes, HLA and other human cell surface
621 antigens-new tools for genetic analysis. *Cell* **14**:9-20.
- 622 27. **Young LS, Lau R, Rowe M, Niedobitek G, Packham G, Shanahan F, Rowe DT, Greenspan D,**
623 **Greenspan JS, Rickinson AB, et al.** 1991. Differentiation-associated expression of the Epstein-
624 Barr virus BZLF1 transactivator protein in oral hairy leukoplakia. *J Virol* **65**:2868-2874.
- 625 28. **Li D, Qian L, Chen C, Shi M, Yu M, Hu M, Song L, Shen B, Guo N.** 2009. Down-Regulation of MHC
626 Class II Expression through Inhibition of CIITA Transcription by Lytic Transactivator Zta during
627 Epstein-Barr Virus Reactivation. *The Journal of Immunology* **182**:1799-1809.
- 628 29. **Zuo J, Hislop AD, Leung CS, Sabbah S, Rowe M.** 2013. Kaposi's sarcoma-associated herpesvirus-
629 encoded viral IRF3 modulates major histocompatibility complex class II (MHC-II) antigen
630 presentation through MHC-II transactivator-dependent and -independent mechanisms:
631 implications for oncogenesis. *J Virol* **87**:5340-5350.

- 632 30. **Tomazin R, Boname J, Hegde NR, Lewinsohn DM, Altschuler Y, Jones TR, Cresswell P, Nelson**
633 **JA, Riddell SR, Johnson DC.** 1999. Cytomegalovirus US2 destroys two components of the MHC
634 class II pathway, preventing recognition by CD4+ T cells. *Nat Med* **5**:1039-1043.
- 635 31. **Johannsen E, Luftig M, Chase MR, Weicksel S, Cahir-McFarland E, Illanes D, Sarracino D, Kieff**
636 **E.** 2004. Proteins of purified Epstein-Barr virus. *Proceedings of the National Academy of Sciences*
637 *of the United States of America* **101**:16286-16291.
- 638 32. **Coscoy L, Ganem D.** 2000. Kaposi's sarcoma-associated herpesvirus encodes two proteins that
639 block cell surface display of MHC class I chains by enhancing their endocytosis. *Proc Natl Acad*
640 *Sci U S A* **97**:8051-8056.
- 641 33. **Ishido S, Wang C, Lee BS, Cohen GB, Jung JU.** 2000. Downregulation of major histocompatibility
642 complex class I molecules by Kaposi's sarcoma-associated herpesvirus K3 and K5 proteins. *J Virol*
643 **74**:5300-5309.
- 644 34. **Ishido S, Goto E, Matsuki Y, Ohmura-Hoshino M.** 2009. E3 ubiquitin ligases for MHC molecules.
645 *Curr Opin Immunol* **21**:78-83.
- 646 35. **Haque M, Ueda K, Nakano K, Hirata Y, Parravicini C, Corbellino M, Yamanishi K.** 2001. Major
647 histocompatibility complex class I molecules are down-regulated at the cell surface by the K5
648 protein encoded by Kaposi's sarcoma-associated herpesvirus/human herpesvirus-8. *J Gen Virol*
649 **82**:1175-1180.
- 650 36. **Lehner PJ, Hoer S, Dodd R, Duncan LM.** 2005. Downregulation of cell surface receptors by the
651 K3 family of viral and cellular ubiquitin E3 ligases. *Immunol Rev* **207**:112-125.
- 652 37. **Brulois K, Toth Z, Wong LY, Feng P, Gao SJ, Ensser A, Jung JU.** 2014. Kaposi's sarcoma-
653 associated herpesvirus K3 and K5 ubiquitin E3 ligases have stage-specific immune evasion roles
654 during lytic replication. *J Virol* **88**:9335-9349.
- 655 38. **Bartee E, McCormack A, Fruh K.** 2006. Quantitative membrane proteomics reveals new cellular
656 targets of viral immune modulators. *PLoS Pathog* **2**.
- 657 39. **Timms RT, Duncan LM, Tchasovnikarova IA, Antrobus R, Smith DL, Dougan G, Weekes MP,**
658 **Lehner PJ.** 2013. Haploid genetic screens identify an essential role for PLP2 in the
659 downregulation of novel plasma membrane targets by viral E3 ubiquitin ligases. *PLoS Pathog*
660 **9**:21.
- 661 40. **Sanchez DJ, Gumperz JE, Ganem D.** 2005. Regulation of CD1d expression and function by a
662 herpesvirus infection. *J Clin Invest* **115**:1369-1378.
- 663 41. **Thomas M, Boname JM, Field S, Nejentsev S, Salio M, Cerundolo V, Wills M, Lehner PJ.** 2008.
664 Down-regulation of NKG2D and NKp80 ligands by Kaposi's sarcoma-associated herpesvirus K5
665 protects against NK cell cytotoxicity. *Proc Natl Acad Sci U S A* **105**:1656-1661.
- 666 42. **Li Q, Means R, Lang S, Jung JU.** 2007. Downregulation of gamma interferon receptor 1 by
667 Kaposi's sarcoma-associated herpesvirus K3 and K5. *J Virol* **81**:2117-2127.
- 668 43. **Bartee E, Mansouri M, Hovey Nerenberg BT, Gouveia K, Fruh K.** 2004. Downregulation of major
669 histocompatibility complex class I by human ubiquitin ligases related to viral immune evasion
670 proteins. *J Virol* **78**:1109-1120.
- 671 44. **Ohmura-Hoshino M, Goto E, Matsuki Y, Aoki M, Mito M, Uematsu M, Hotta H, Ishido S.** 2006.
672 A novel family of membrane-bound E3 ubiquitin ligases. *J Biochem* **140**:147-154.
- 673 45. **Ohmura-Hoshino M, Matsuki Y, Aoki M, Goto E, Mito M, Uematsu M, Kakiuchi T, Hotta H,**
674 **Ishido S.** 2006. Inhibition of MHC class II expression and immune responses by c-MIR. *J Immunol*
675 **177**:341-354.
- 676 46. **Hoer S, Smith L, Lehner PJ.** 2007. MARCH-IX mediates ubiquitination and downregulation of
677 ICAM-1. *FEBS Lett* **581**:45-51.

678 47. **Nathan JA, Lehner PJ.** 2009. The trafficking and regulation of membrane receptors by the RING-
679 CH ubiquitin E3 ligases. *Exp Cell Res* **315**:1593-1600.

680 48. **Fogg MH, Carville A, Cameron J, Quink C, Wang F.** 2005. Reduced prevalence of Epstein-Barr
681 virus-related lymphocryptovirus infection in sera from a new world primate. *J Virol* **79**:10069-
682 10072.

683 49. **Wang F.** 2013. Nonhuman primate models for Epstein-Barr virus infection. *Curr Opin Virol*
684 **3**:233-237.
685
686

687 **Funding Information:**

688 This work was supported by grants from the Medical Research Council, London, UK
689 (G0901755). The funders had no role in study design, data collection and interpretation,
690 or the decision to submit the work for publication.

691

692 **Acknowledgments:** We thank for Dr Andrew Hislop for helpful discussions during this
693 study.

694

695 **Figure legends**

696 **Figure 1. Screening of EBV lytic genes to identify potential MHC class I immune**
697 **evasion genes.** MJS cells were transiently transfected with pCDNA3.1-IRES-GFP
698 plasmids encoding for a selection of EBV lytic genes. At 24h post transfection surface
699 levels of MHC class I (A) and MHC class II (B) on GFP positive cells were analysed
700 using two color flow cytometry. (C) AKBM cells were induced into lytic cycle by cross-
701 linking of B cell receptors for 1hr at 37°C and analyzed at time points post-induction, as
702 indicated, using western blot. Levels of BZLF1 protein (upper blot), BDLF3 protein
703 (middle blot; stars indicate monomeric and trimeric BDLF3 protein) and, as a loading
704 control, calregulin (lower blot) are shown.

705 **Figure 2. BDLF3 expression induces the down regulation of surface MHC class I**
706 **and MHC class II.** MJS cells (A-D) and DG75 cells (E-H) were transiently transfected
707 with control-GFP or BDLF3-GFP plasmids. At 24h post transfection, two color flow
708 cytometry was used to measure surface levels of MHC class I (A,E), MHC class II (B,F),
709 TfR (C,G) and ICAM1 (D) or CD19 (H) in the GFP⁺ populations of control-GFP (solid
710 line histogram), and BDLF3-GFP transfected cells (dashed line histogram). The grey
711 histogram denotes background staining obtained with an isotype control antibody.

712 **Figure 3. BDLF3 induces downregulation of all HLA class I and class II alleles.** (A)
713 The MHC class I negative cell line K562 transduced to stably express either HLA-A2, -
714 B35 or -Cw1 was electroporated with control-GFP or BDLF3-GFP plasmids. At 24h
715 post-transfection, two color flow cytometry was used to measure surface MHC class I
716 levels in the GFP⁺ populations in the control-GFP transfected (solid line histogram) and

717 the BDLF3-GFP transfected cells (dashed line). (B) HEK-293 cells stably expressing
718 CIITA were transiently transfected with control-GFP or BDLF3-GFP plasmids. At 24h
719 post-transfection, two color flow cytometry was used to measure surface HLA-DR and
720 HLA-DQ levels in GFP⁺ populations in the control-GFP transfected (solid line histogram)
721 and the BDLF3-GFP transfected cells (dashed line). The grey histogram denotes
722 background staining obtained with an isotype control antibody.

723 **Figure 4. BDLF3 can inhibit EBV specific CD8⁺ and CD4⁺ T cell recognition.** MJS
724 cells were co-transfected with p509 plasmid (BZLF1 expression vector) together with
725 control-GFP or BDLF3-GFP. At 24h post transfection, the MJS cells were co-cultured
726 with effector T cells, BZLF1 (RAK)-specific CD8⁺ T cell clone, for a further 18hr and the
727 supernatants were tested for the release of IFN- γ as a measure of T cell recognition. All
728 results are expressed as IFN- γ release in pg/ml and error bars indicate standard
729 deviation of triplicate cultures. (B) Total cell lysates were generated from the above
730 transfections, and analyzed by western blotting using antibodies specific for BDLF3,
731 BZLF1 or calregulin as a loading control. The asterisks adjacent to the BDLF3 blot
732 indicate monomeric and trimeric BDLF3 protein. (C) MJS-DR51 cells were first
733 transfected with EBNA1 Δ NLS, allowed to recover in culture overnight, then were divided
734 to two groups and transfected with either BDLF3-NGFR or Control-NGFR. After a
735 further 24h, NGFR⁺/BDLF3⁺ or control NGFR⁺ cells were sorted with magnetic beads
736 and used as targets for HLA-DR51 restricted EBNA1 (SNP) specific CD4⁺ T cell clones.
737 Recognition was measured as pg/ml of IFN- γ release by T cell clones. Error bars
738 represent standard deviation of the mean for triplicate assay replicates. Results are

739 representative of three independent experiments. (D) Total cell lysates were generated
740 from the above transfections, and analyzed by western blotting using antibodies specific
741 for BDLF3, EBNA1 or calregulin as a loading control.

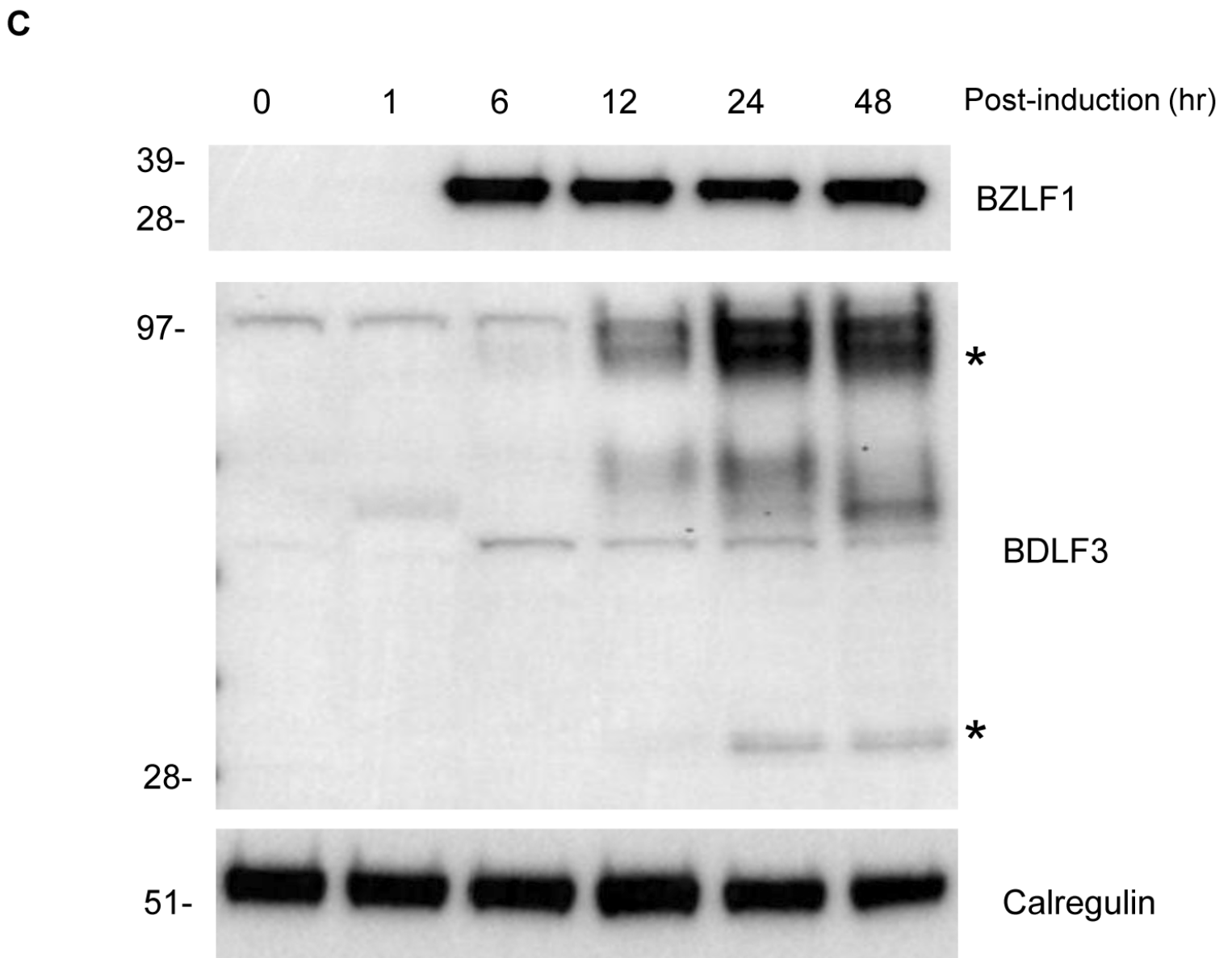
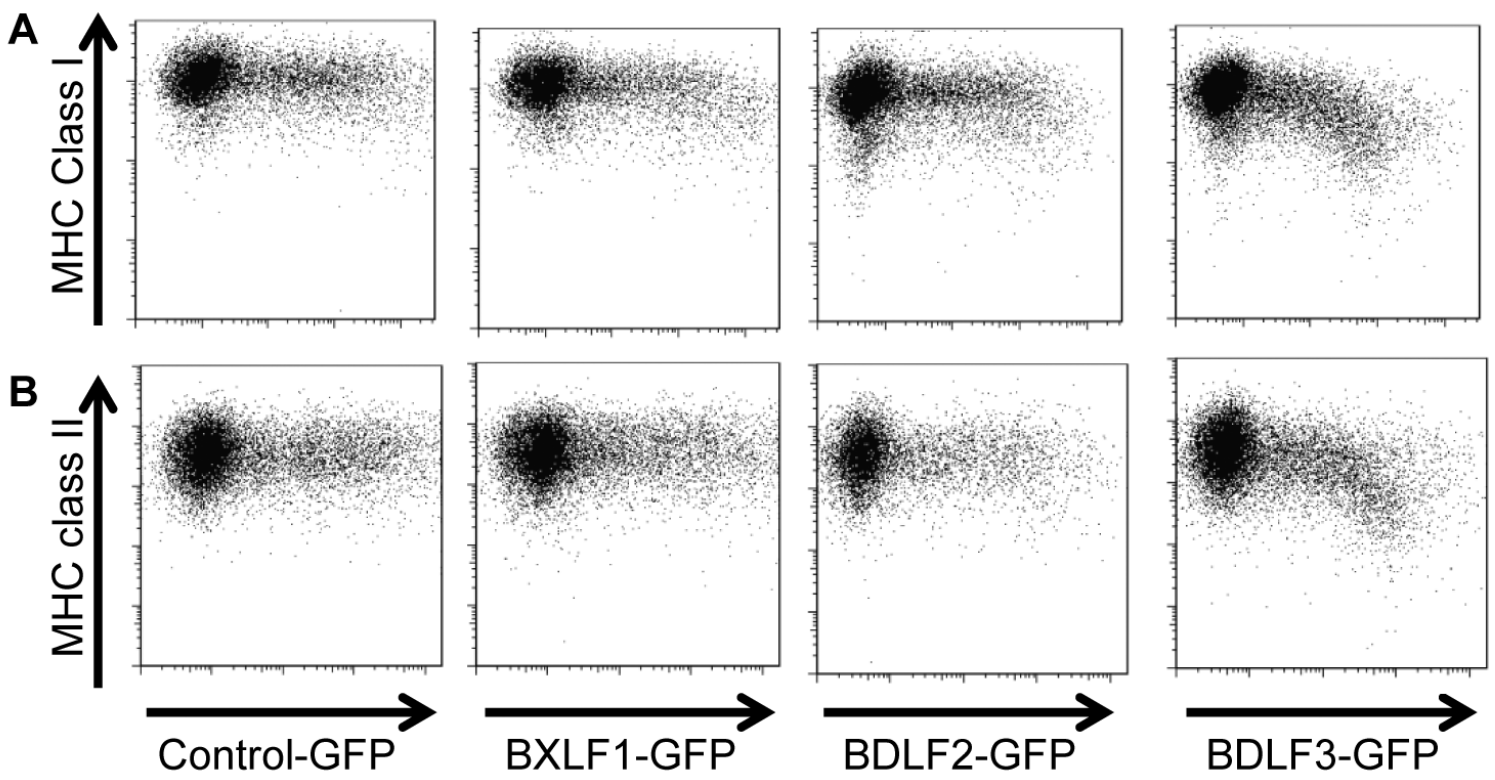
742 **Figure 5. BDLF3 induces a more dramatic reduction in surface MHC class I and II**
743 **compared to whole cell levels.** (A) MJS cells were transiently transfected with control-
744 GFP or BDLF3-GFP plasmids. At 24h post transfection, two color flow cytometry was
745 used to measure the level of surface MHC class I (upper left), MHC class II (middle left)
746 and ICAM1 (lower left) in the viable GFP⁺ populations of control-GFP transfected (solid
747 line histogram), and BDLF3-GFP transfected cells (dashed line histogram). The grey
748 histogram denotes background staining obtained with an isotype control antibody. In
749 parallel, these GFP⁺ transfected MJS cells were analysed for whole cell levels of MHC
750 class I (upper right), MHC class II (middle right) and ICAM1 (lower right) using
751 intracellular staining of fixed and permeabilized cells. The results are representative of
752 repeated experiments. (B) Relative mean fluorescence intensity (MFI) of MHC class I,
753 MHC class II and ICAM1 in BDLF3-GFP⁺ cells compared to control-GFP⁺ cells were
754 calculated. Results are the combined data from three independent experiments. White
755 bars represent surface staining, grey bars represent whole cell staining. Differences that
756 reached significance ($p < 0.05$) in a Student's Paired T test are denoted by an asterisk.

757 **Figure 6. BDLF3 induces more rapid internalization and delayed appearance of**
758 **both MHC class I and class II at the cell surface.** Internalization and appearance
759 assays were performed on MJS cells transiently expressing control-GFP or BDLF3-
760 GFP. The GFP⁺ population was used to gate on BDLF3 expressing cells. Internalization

761 and appearance assays were performed on cells pre-treated on ice with saturating
762 amounts of anti-MHC class I antibody or anti-MHC class II antibody. Cells were then
763 washed and incubated at 37°C for up to 60 min. (A) For the internalization assay, viable
764 cells harvested at each time point were stained with APC-conjugated goat anti-mouse
765 IgG antibody, and analyzed using flow cytometry at the indicated times; this identifies
766 the pre-labeled antibody-bound MHC molecules that remain at the surface while
767 endocytosed labeled MHC molecules are not detected on the viable cells. The mean
768 fluorescence intensities of staining were averaged for triplicate samples, and then
769 normalized to the time 0 samples. (B) For the appearance assays, newly-arrived MHC-I
770 and MHC-II molecules, which were not pre-labeled with unconjugated antibodies, were
771 detected by staining with APC-conjugated anti-MHC class I antibody or anti-MHC class
772 II antibody. The mean fluorescence intensities of staining were averaged for triplicate
773 samples, and then normalized to the time 0 samples. Results are representative of
774 three independent experiments.

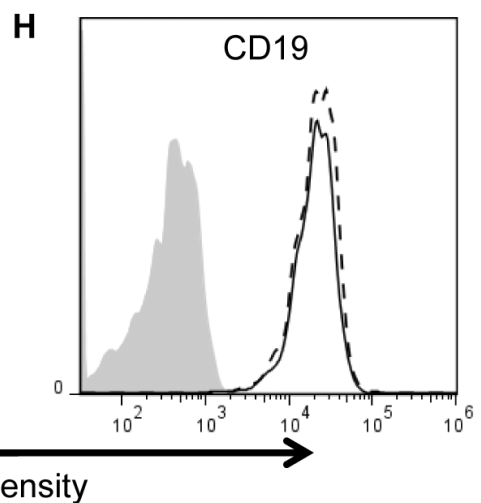
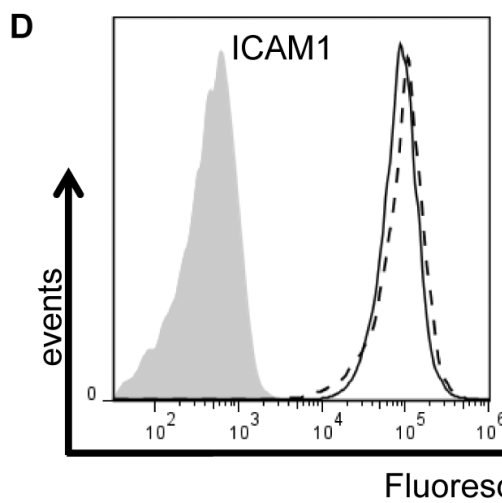
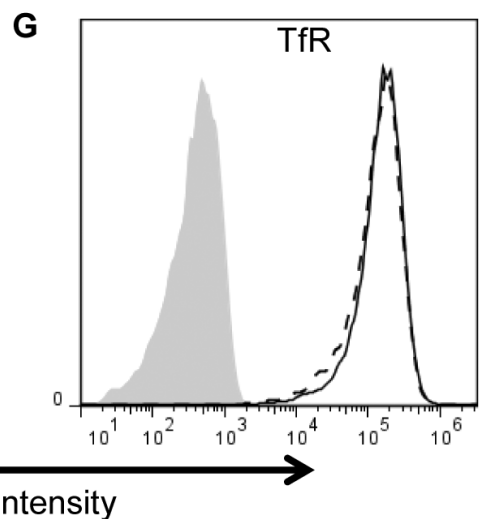
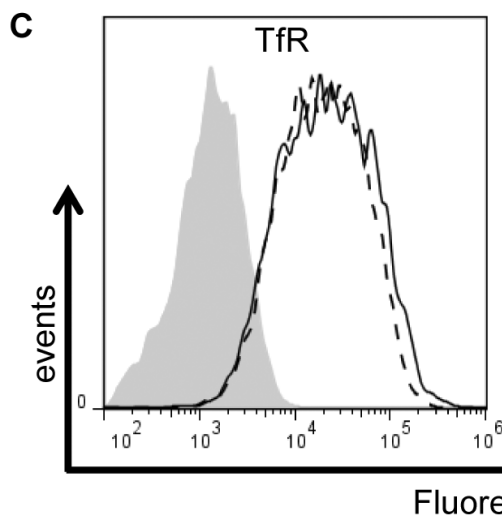
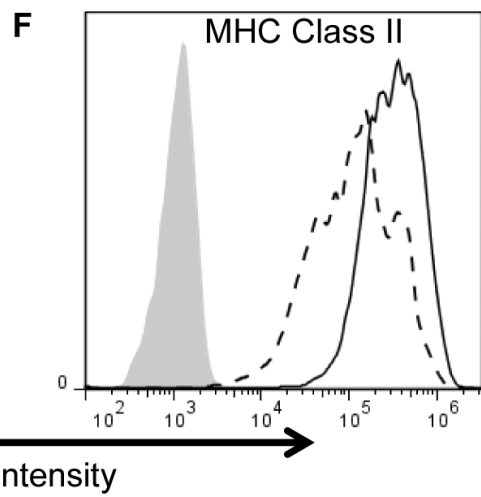
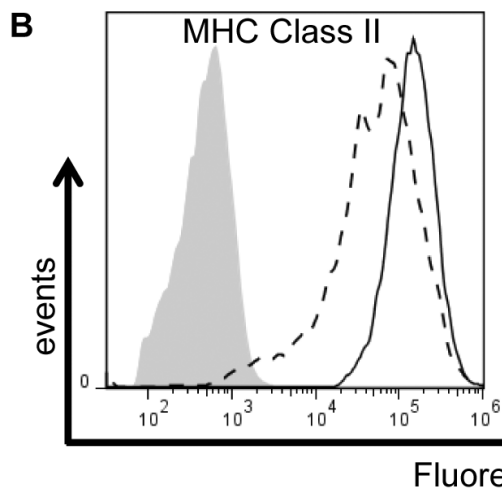
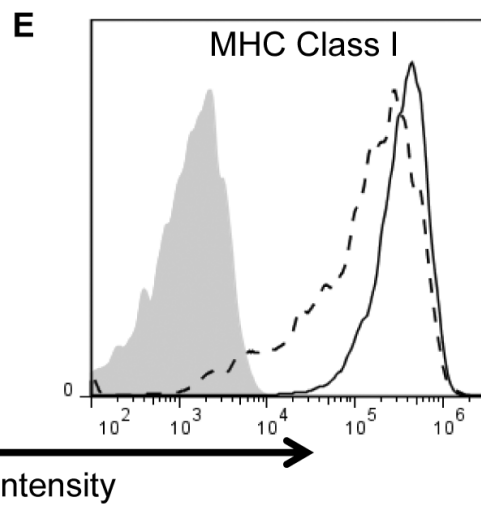
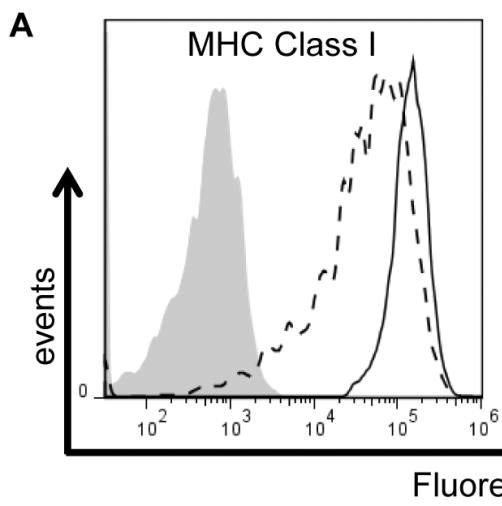
775 **Figure 7. Treatment of BDLF3 expressing cells with a proteasome inhibitor**
776 **prevents down regulation of MHC class I and class II.** MJS cells were transiently
777 transfected with BDLF3-GFP or control-GFP plasmids, and then incubated in normal
778 medium (A) or with MG132 (5µM) supplemented medium (B). At 24h post-transfection,
779 two color flow cytometry was used to measure surface MHC class I (upper histograms),
780 surface MHC class II (middle histograms) and surface ICAM1 (lower histograms) in
781 GFP⁺ populations of control-GFP (solid line histogram), and BDLF3-GFP (dashed line
782 histogram) transfected cells. The grey histogram denotes background staining obtained

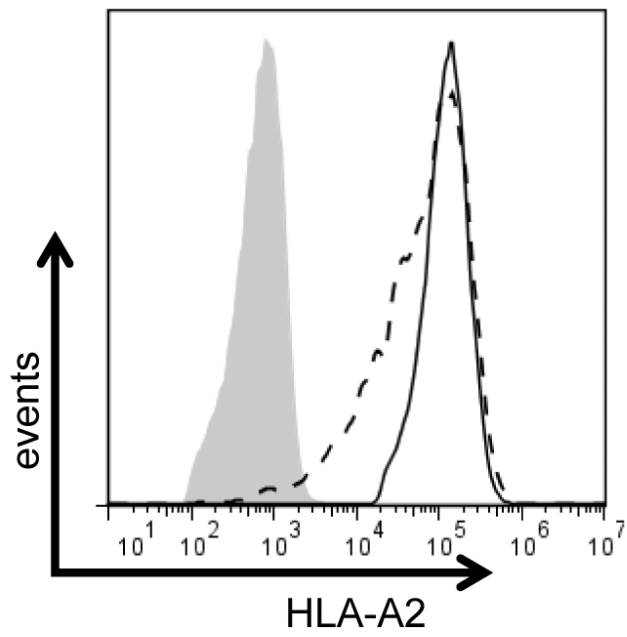
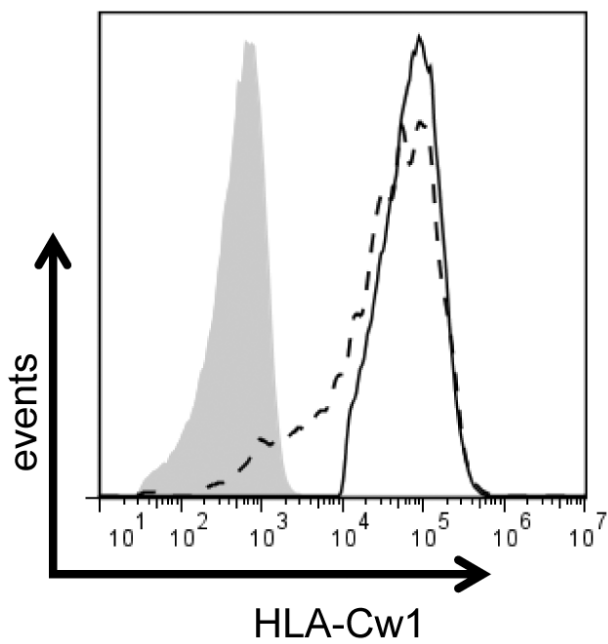
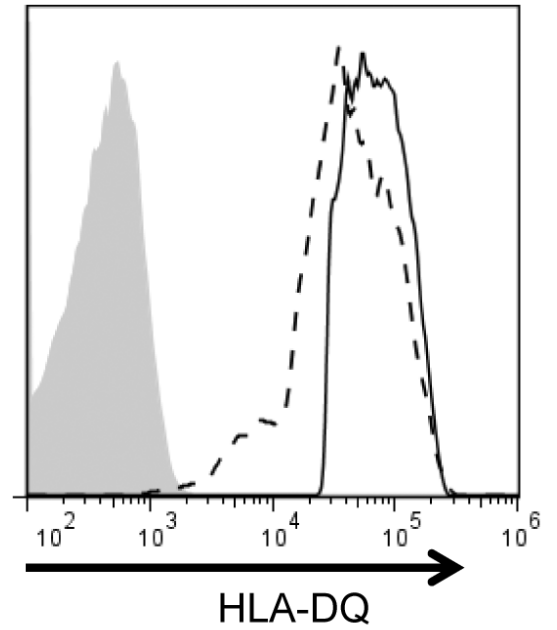
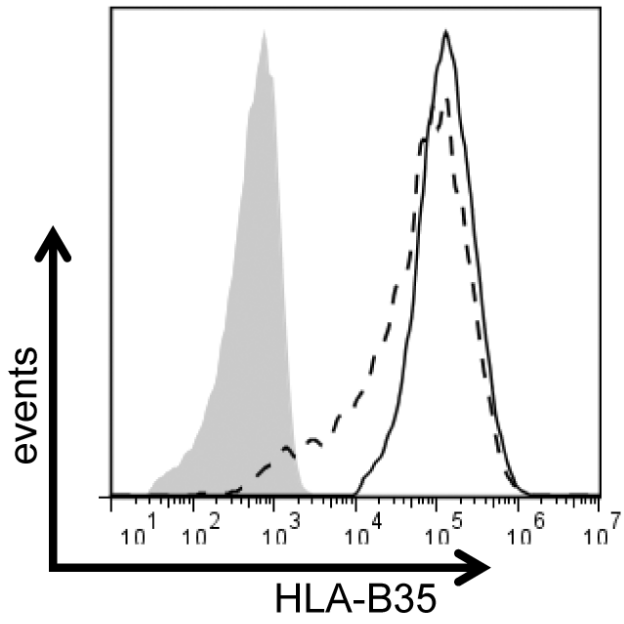
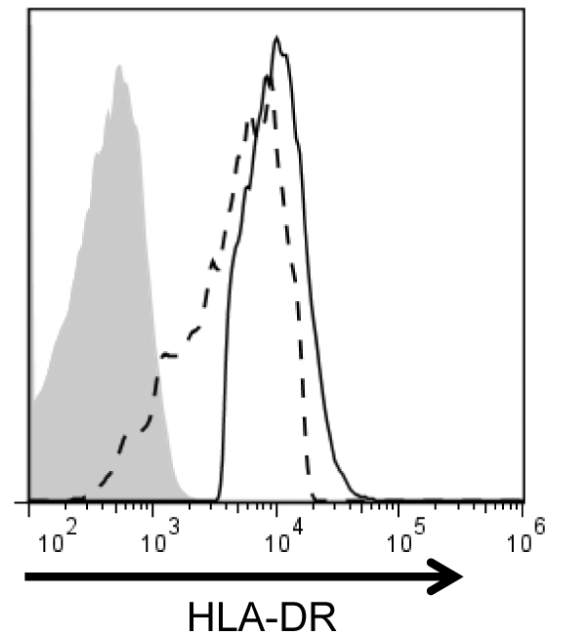
783 with an isotype control antibody. Results are representative of repeated experiments
784 (n>4). (C,D) MJS cells were transiently transfected with BDLF3-GFP or control-GFP
785 plasmids, and then were incubated with MG132 (5 μ M). Following drug treatment, the
786 rate of internalization (C) of MHC-I (top panel) and MHC-II (bottom panel), and the rate
787 of appearance (D) of MHC-I (top panel) and MHC-II (bottom panel) were measured
788 using the same method as in Fig. 6. (E, F) MJS cells were transfected with a ubiquitin
789 expression plasmid plus either Control-NGFR or BDLF3-NGFR plasmids; these
790 transfected cells were then divided in to two and incubated in normal medium or in
791 medium supplemented with MG132. At 24h post transfection, NGFR⁺/BDLF3⁺ or control
792 NGFR⁺ cells were sorted with magnetic beads, and surface MHC class I (C) or MHC
793 class II (D) were immunoprecipitated, eluted, and then immunoblotted using anti-
794 ubiquitin antibody (P4D1).

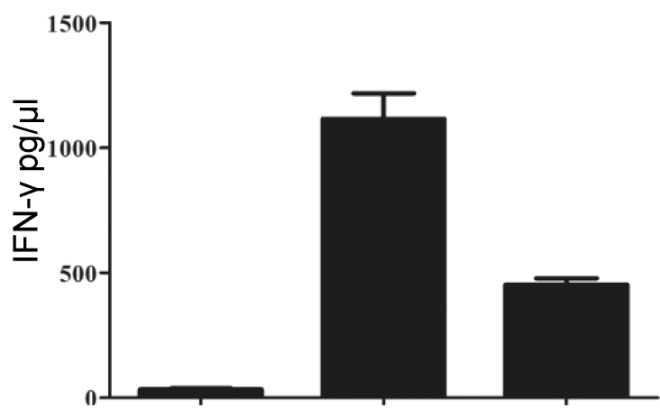
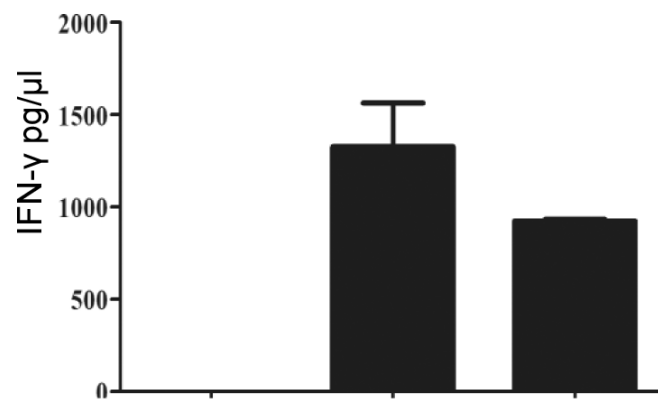


MJS

DG75



A**B**

A**C**

BDLF3

-

-

+

BDLF3

-

-

+

BZLF1

-

+

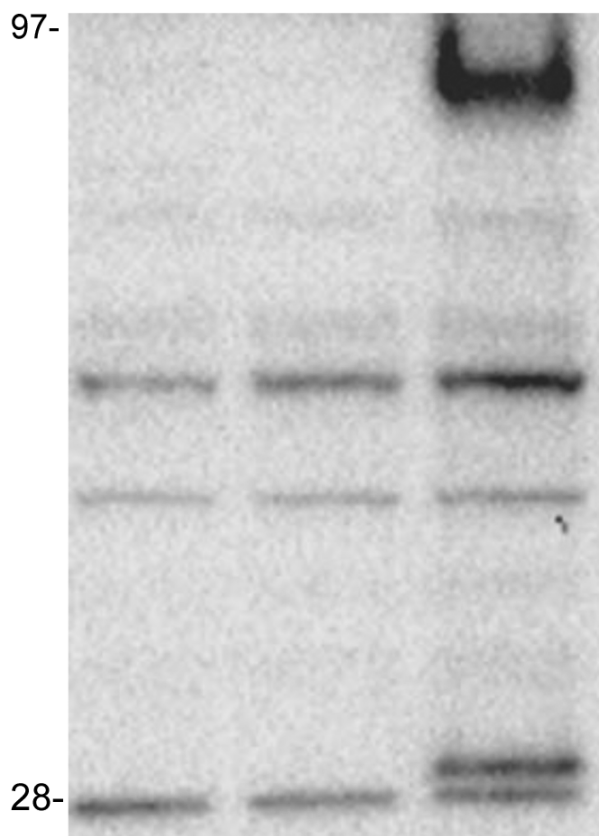
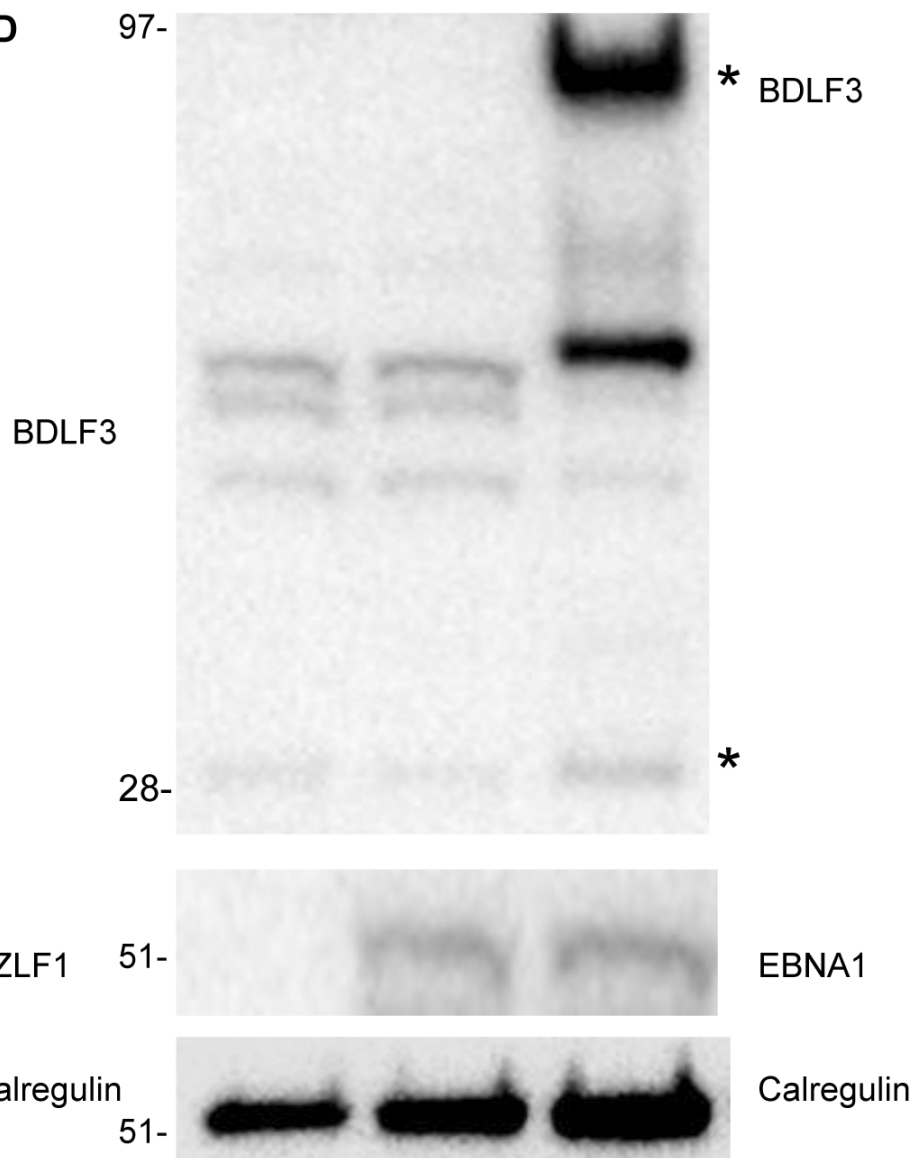
+

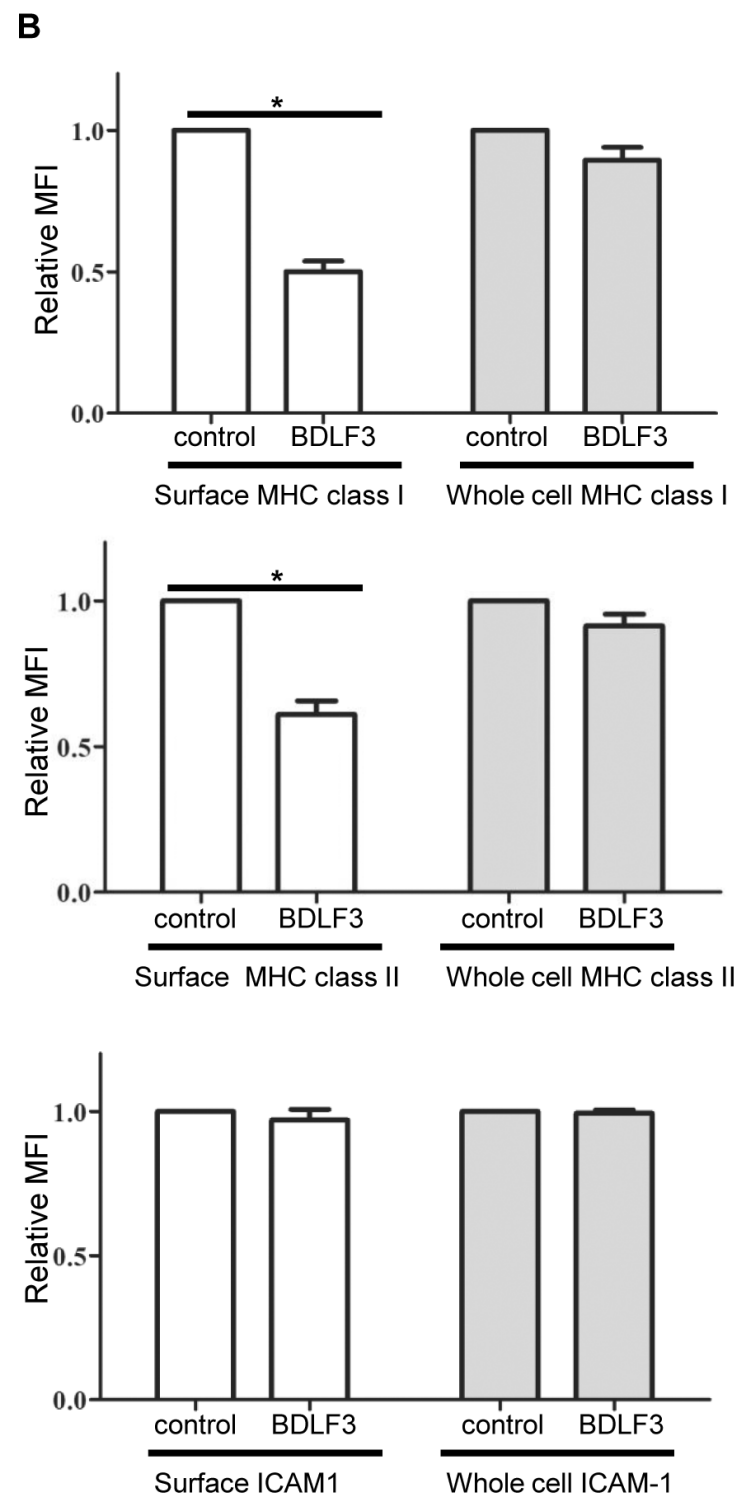
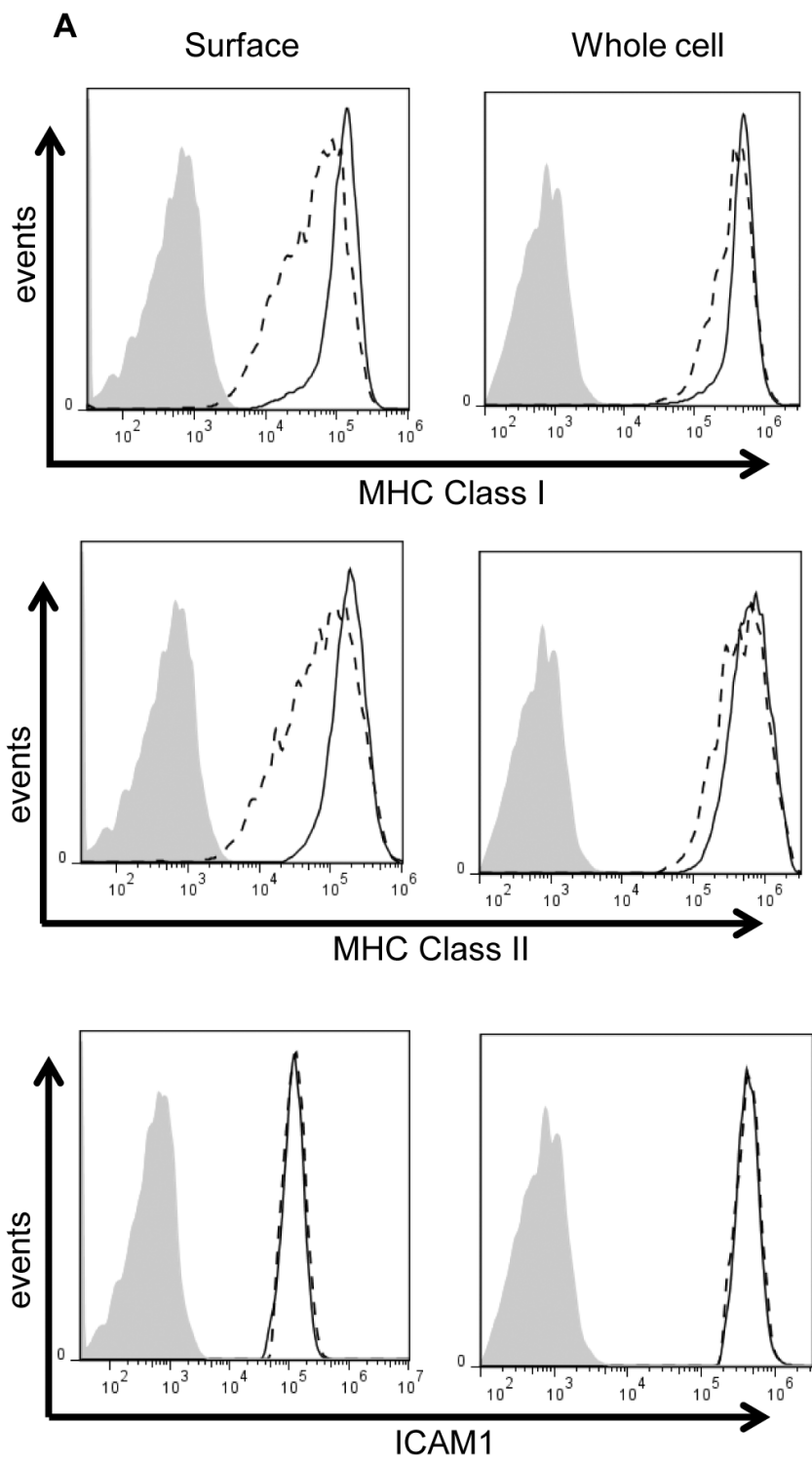
EBNA1

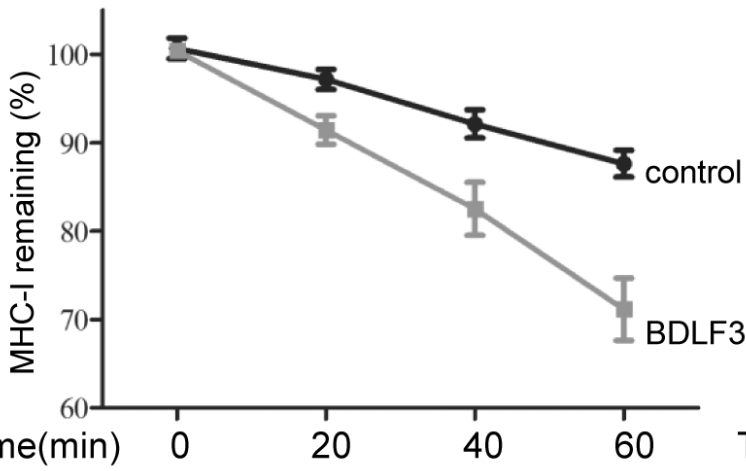
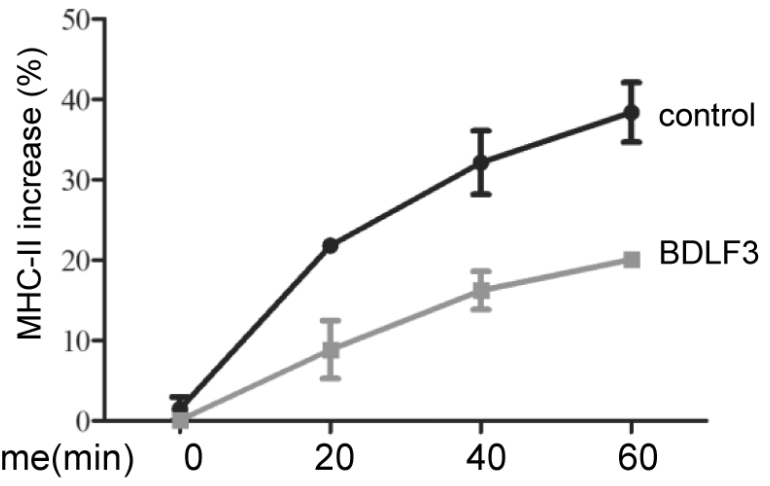
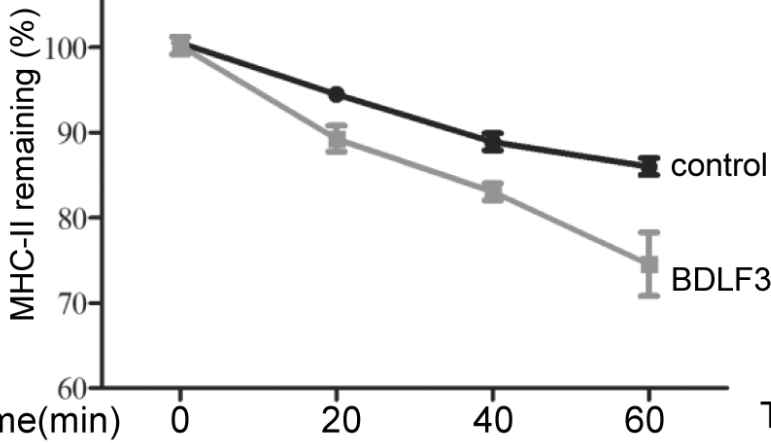
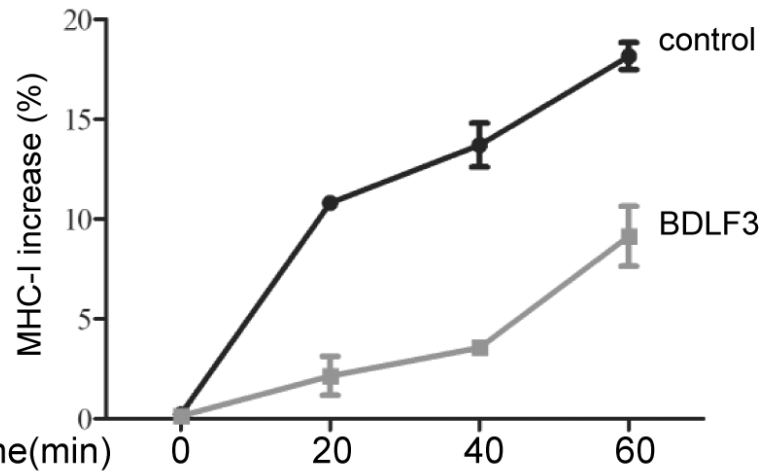
-

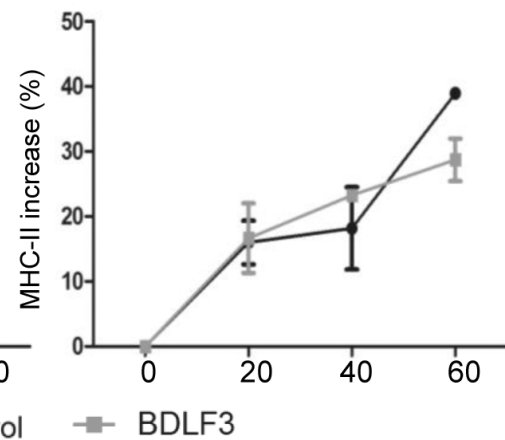
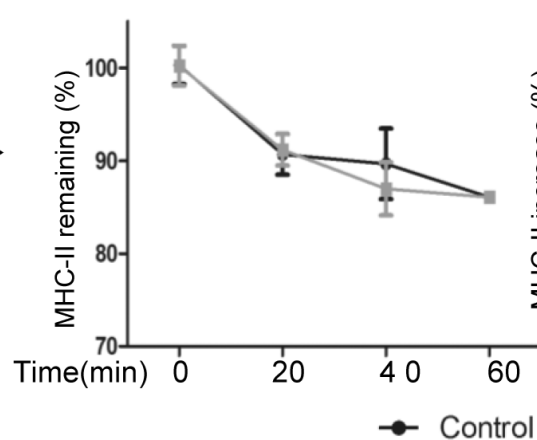
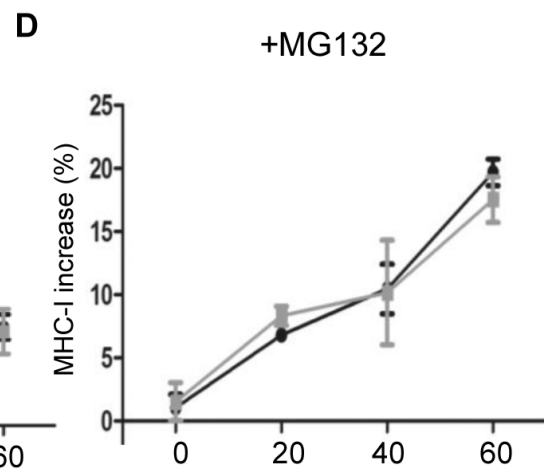
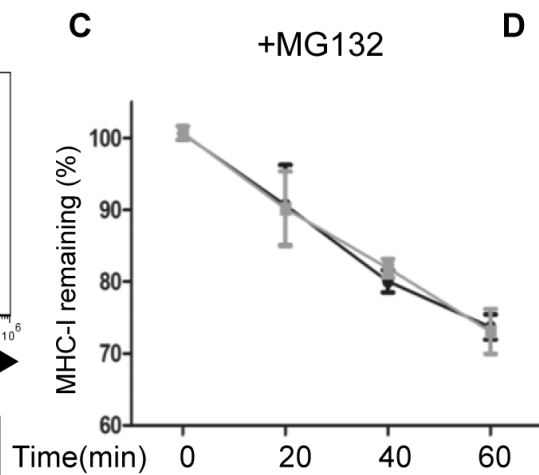
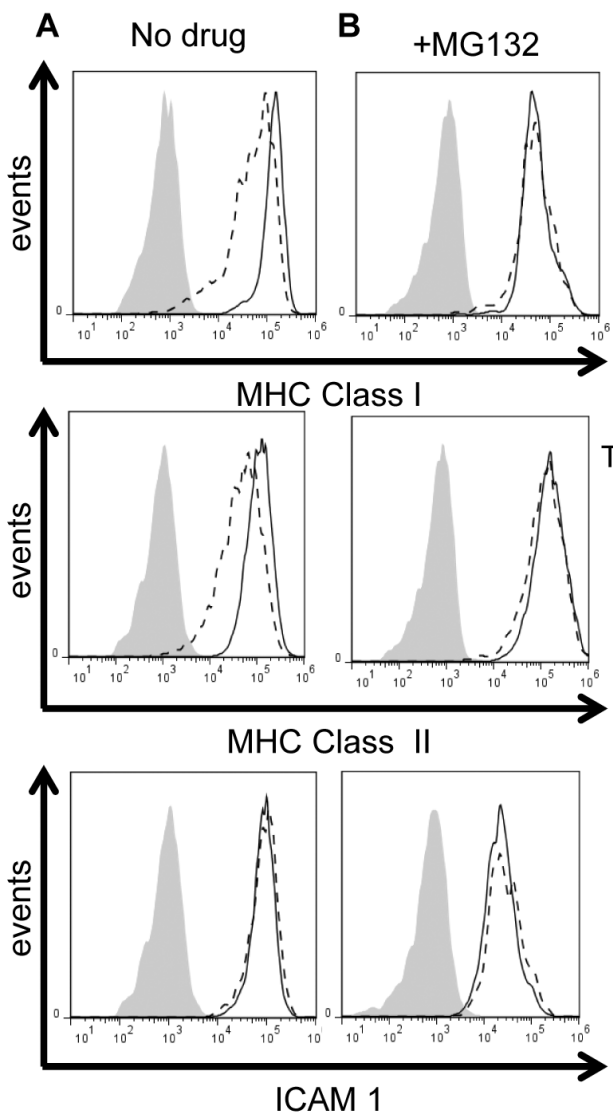
+

+

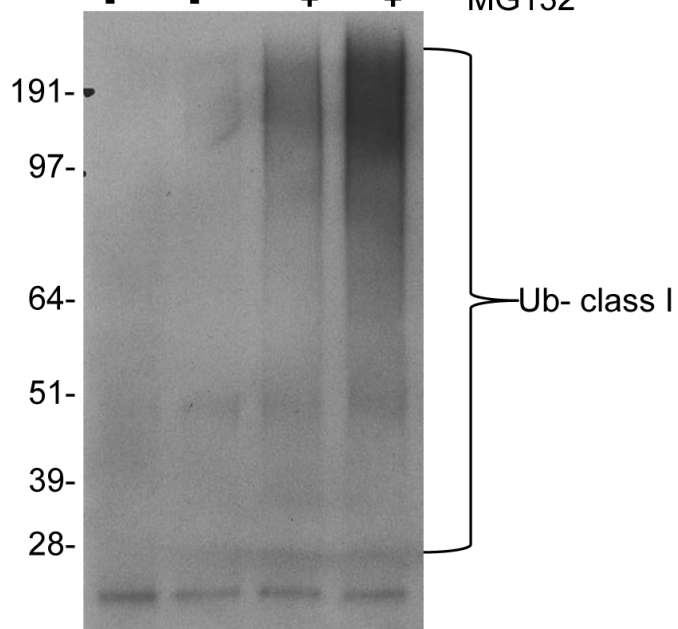
B**D**



A**B**



E - + - + BDLF3
 - - + + MG132



F - + - + BDLF3
 - - + + MG132

